NASA Technical Memorandum 78683

EFFECT OF LEADING-EDGE CONTOUR AND VERTICAL-TAIL CONFIGURATION ON THE LOW-SPEED STABILITY CHARACTERISTICS OF A SUPERSONIC TRANSPORT MODEL HAVING A HIGHLY-SWEPT ARROW WING

VERNARD E. LOCKWOOD

March 1978

National Aeronautics and Space Administration

Langley Research Center
Hampton, Virginia 23665

NATIONAL AERONAUTICS AND SPACE ADMINISTRATION

EFFECT OF LEADING-EDGE CONTOUR AND VERTICAL-TAIL CONFIGURATION ON THE LOW-SPEED STABILITY CHARACTERISTICS OF A SUPERSONIC TRANSPORT MODEL HAVING A HIGHLY-SWEPT ARROW WING

By Vernard E. Lockwood
Langley Research Center
Hampton, Virginia

SUMMARY

A low-speed investigation has been made on a highly-swept arrow-wing model to determine the effect of wing leading-edge contour and vertical-tail configuration on the aerodynamic characteristics in pitch and sideslip. The investigation was made with the trailing-edge flaps deflected over a range of angles of attack from 8° to 32°. The tests were made at a Mach number of 0.13, which corresponds to a Reynolds number of about 3×10^{6} based on the wing reference chord.

The results showed the basic wing configuration had a pitch-up tendency that began about 11°, a modification to the wing which increased the leading-edge radius and camber extended the angle for pitchup to 19°. A leading-edge flap used in combination with the greater radius practically eliminated the pitch-up tendency. The modified leading edges resulted in favorable increases in the lift-drag ratio and undesirable

increases in the angle of attack and pitching-moment coefficient for a given lift coefficient. The presence of the outboard vertical tails caused a loss of lift which was destabilizing in pitch, but the use of the vertical tails with the basic wing provided good directional stability. The thickened leading edge reduced the directional stability for all vertical-tail configurations and the directional stability was decreased even more by deflection of the leading edge. Positioning the outboard vertical tails above the engine nacelles reduced both the longitudinal and directional stability. A forebody strake in combination with a relatively small centerline vertical tail provided directional stability to a lift coefficient of 1.35.

The modified leading edges caused large reductions in dihedral effect with the outboard vertical tails off, however, above lift coefficients of 0.6 there was little difference in dihedral effect.

INTRODUCTION

The National Aeronautics and Space Administration has made studies of various aerodynamic configurations over the past several years in support of the supersonic transport program. One configuration which appears highly promising from supersonic considerations is the blended wing-body concept which is described in reference 1. Results of an investigation at transonic speeds (reference 2) have indicated the configuration was longitudinally stable at Mach numbers greater than 0.97 but exhibited decreasing stability (pitch-up tendencies) as the Mach number was decreased to 0.5. Low-speed tests of this configuration

designated, SCAT-15F , indicated a complete loss of longitudinal stability at lift coefficients above 0.2. The loss in stability was partially controlled with aid of leading-edge flaps. The design utilized upward deflecting trailing-edge flaps for trim at high-lift coefficients. This arrangement resulted in low lift-drag ratios and undesirable high angles of attack for landing and take-off attitudes. Additional research was conducted on this configuration utilizing positive lift trailing-edge flaps in conjunction with a canard for longitudinal trim, the results, however, were generally unsatisfactory as indicated in reference 4.

The original 15F configuration was redesigned in 1968 to incorporate changes which were expected to improve the low-speed performance without serious penalties to the high-speed potential. The redesigned version (SCAT 15F-9898) when compared to the original 15F had increased size, decreased sweep of the wing trailing edge, and increased wing leading-edge radius. The later version also incorporated wing leading-edge flaps, a ventral fin, and a small horizontal tail for longitudinal control. Several low-speed investigations were made with the later version (0.03-scale model), the results of which are reported in references 5 to 10. It was observed in the initial investigation (reference 5) that the pitch-up tendency evident in the earlier investigations of SCAT 15F was still prevalent in the 15F-9898 version, although materially reduced. Considerable effort was spent in trying to reduce the pitch-up tendency through the use of thicker leading edges and larger more effective horizontal tails. One possible configuration is illustrated in figure 8 of reference 9 in which a thick

leading edge was used in conjunction with a leading-edge flap, a large horizontal tail, and a lengthened aft fuselage. These data were obtained at relatively low Reynolds numbers. An earlier investigation (reference 10) has indicated the pitch-up tendency may be a function of Reynolds number and has indicated the possibility of reducing the overall pitch-up moments by increasing the leading-edge Reynolds number either through increasing the leading-edge radius or the flow Reynolds number.

In the efforts to improve the longitudinal characteristics little attention was given to determine the effect of configuration changes on the lateral characteristics. It is apparent, however, from characteristics determined in sideslip that the directional stability can be adversely affected by changes in leading-edge geometry. For example, the data of reference 5 shows negative values of the directional-stability parameter, C_{n_β}, exist above 9° angle of attack with the leading edge deflected. The data of reference 6, however, show no losses for the undeflected leading edge, but show increasing values of C_{n_β} to 22° angle of attack. The large difference in the directional characteristics suggests that additional research is needed on highly swept wings to avoid compromising the directional stability to obtain desirable pitch characteristics.

The present investigation was initiated to provide some insight into the effect of leading-edge configurations on the aerodynamic characteristics in sideslip. Three leading-edge configurations were tested in combination with several vertical-tail configurations. Lateral-stability parameters were computed from the tests made at sideslip angles of $\pm 5^\circ$ for an angle-of-attack range from about 8° to 32°. The corresponding longitudinal coefficients are also included.

SYMBOLS

The data are referred to the stability-axis system with the moments referenced to the point shown in figure 1, which corresponds to $0.456\bar{c}$. The symbols are defined as follows:

C_D	drag coefficient, $\frac{\text{Drag}}{qS}$
C_L	lift coefficient, $\frac{\text{Lift}}{qS}$
C_ℓ	rolling-moment coefficient, $\frac{\text{Rolling moment}}{qSb}$
C_{ℓ_β}	effective dihedral parameter, $\frac{\Delta C_\ell}{\Delta\beta}$, per deg
C_m	pitching-moment coefficient, $\frac{\text{Pitching moment}}{qS\bar{c}}$
C_n	yawing-moment coefficient, $\frac{\text{Yawing moment}}{qSb}$
C_{n_β}	directional-stability parameter, $\frac{\Delta C_n}{\Delta\beta}$, per deg
$\Delta C_{n,t}$	incremental yawing-moment coefficient due to the addition of vertical tails
C_Y	side-force coefficient, $\frac{\text{Side force}}{qS}$
C_{Y_β}	side-force parameter, $\frac{\Delta C_Y}{\Delta\beta}$, per deg
L/D	lift-drag ratio

Reference Dimensions:

A	aspect ratio, $\frac{b^2}{S}$, 1.624
b	wing span, 45.648 in.
$\bar{c}$	wing chord, 38.310 in.
q	free-stream dynamic pressure
S	wing area, 8.908 sq ft (See figure 1 of reference 5.)

Model Component Designations (See figures 1 to 9.):

B_9	body (short nose and extended fuselage)
c	local wing chord
E_2	engine nacelles
f_2	forebody strake
H_4	horizontal tail
$L_{1,2,3}$	leading-edge flap
L_6	wing tip flap
N_2	notch at wing-fuselage juncture
t	trailing-edge flaps ($t_{1,f} = t_2 = t_3 = 2^0$, $t_4 = 5^0$)
$t_{1,f}$	t_1 extended to represent a fowler flap
$V_{23,I}$	inboard vertical tail
$V_{23,O}$	outboard vertical tail
V_4	centerline vertical tail
V_6	ventral fin and rudder
W_1	basic leading edge (radius = 0.002c)
W_3	modified leading edge (radius = 0.010c)
$W_{3=30^0}$	modified leading edge deflected 30^0

Angular Designations:

α	angle of attack of wing reference line, deg
β	angle of sideslip, deg

MODEL AND SUPPORT

The model used in the investigation is a modification of the basic arrow planform described in references 1 to 6. These modifications include revisions to the wing planform, wing dihedral, fuselage and model support. A three-view drawing of the model is shown in figure 1 and a photograph of the model and support system is shown in figure 2. An overhead sting, coupling, and balance adapter were utilized in order that a ventral fin could be used with a closed afterbody. The offset coupling was provided with a free floating fairing to reduce the wake effects. The fuselage, designated B_9 , which originated with a drooped nose at station 5.0 (see figure 3) was 108 inches long ending with an closed fuselage at station 113 as shown in figure 1.

The wing had a broken leading edge with sweep angles starting inboard of 74.0°, 70.5°, and 60.0° and trailing-edge sweep angles of 0.0°, 24.0°, and 36.7°, respectively. A longitudinal cut at spanwise station 5.8 inches provided a means of obtaining 4° of anhedral compared to the model reported on in references 1 to 6.

The leading edge of the wing was equipped with a notch, N_2 , a leading-edge flap, L_{1-3} , and a chord extension on the wing tip as shown in figure 4. The basic leading-edge contour, W_1 , and the modified contours, W_3 , shown in figure 5 extended to spanwise station 18.40; flap $W_3 = 30^\circ$ extended to station 12.39. Details of the trailing-edge flaps, t_1, t_2, and t_3 , which were deflected 20° are shown in figures 4 and 6. (The flap designated, t_4 , in figure 4 was undeflected for the investigation.)

The horizontal tail, H_4 , which was used throughout the investigation is shown in figure 7.

Three vertical-tail configurations were used in the investigation and these are illustrated in figure 8. Vertical tail, V_{23} , was tested in two spanwise locations on the wings as shown in figure 4. Because of the wing trailing-edge sweep the V_{23} was located farther forward at the inboard location, $V_{23,i}$, than at the outboard location, $V_{23,o}$. Vertical tail, V_6 and V_4 , are shown in figures 8(b) and 8(c), respectively.

Drawings of the inboard and outboard engine nacelles, E_2 , are presented in figure 9. Additional information on the model components is presented in Table I.

TEST CONDITIONS

The investigation was conducted in the Langley high-speed 7- by 10-foot tunnel which is an atmospheric facility. The tunnel has a closed test section with a cross-sectional area of 63 square feet.

The investigation was made at a dynamic pressure of 25 pounds per square foot which corresponds to a Mach number of 0.13 and a Reynolds number of 3.0×10^6 based on the wing reference chord. A one-tenth inch wide strip of No. 80 carborundum was placed about 1 inch aft of the leading edge of all model components to insure turbulent flow in the model boundary layer. The transition grit was also included on the inside surface of the engine nacelles.

MEASUREMENTS AND CORRECTIONS

The aerodynamic forces and moments were measured by a six-component, electrical strain-gage balance housed within the model. The angles of attack were measured directly by means of an accelerometer attached to the model.

Jet-boundary and blockage corrections calculated by the method of references 11 and 12, respectively, have been applied to the data with the exception of the jet-boundary correction to the pitching moments. Recent tests have indicated a small correction should be applied to these data in the higher angle-of-attack range. The correction would tend to make the pitching moments slightly more positive. In addition, adjustments have also been made to the drag coefficients to account for the internal skin-friction drag of the nacelles (a drag increment of 0.0010 has been subtracted from the total drag coefficient of the model). No tares have been applied to the data to account for support strut interference effects on the model.

PRESENTATION OF DATA

The data obtained in the investigation are presented in the following figures:

DISCUSSION

Longitudinal Characteristics

Only angle-of-attack runs at $\pm 5^{\circ}$ sideslip were made since the primary purpose of the investigation was to study the lateral-directional characteristics. However, one configuration was tested at 0° and $\pm 5^{\circ}$ so that the effect of sideslip angle on the longitudinal characteristics might be evaluated. The results of these tests are presented in figure 10 for the basic wing configuration, W_1 . It will be noted that the longitudinal coefficients obtained at $\pm 5^{\circ}$ sideslip represent quite closely the data obtained at 0°. Because of the similarity in the longitudinal coefficients shown in figure 10, it would appear valid to use other sideslip data for an evaluation of the longitudinal characteristics.

The effect of wing leading-edge configuration on the longitudinal characteristics are presented in figure 11 for several vertical-tail arrangements. The basic leading edge, W_1 , shows, as would be expected from previous experience, a pitch-up tendency (dC_m/dC_L increases positively as C_L increases) beginning at 12° angle of attack. A change from leading edge W_1 to W_3 increased the angle of attack for pitchup to about 19° and reduced the overall pitch-up tendency. A 30° deflection of leading-edge flap, W_3 , eliminated the pitch-up tendency with vertical tails removed as shown in figure 11(a).

The use of leading edges W_3 and $W_3 = 30^\circ$ in place of W_1 for reducing the pitch-up tendency resulted in favorable increases in the lift-drag ratio and undesirable increases in the angle of attack and pitching-moment coefficients for a given lift coefficient. For example, the data shown in figure 11(d) for the outboard vertical tail indicates that at a lift coefficient of 0.58, W_3 showed a 10-percent increase in lift-drag ratio, a 1° increase in angle of attack over W_1 and an increase in the out-of-trim pitching-moment coefficient of 0.011. Except for the reduction in pitch-up tendency the characteristics obtained with $W_3 = 30^\circ$ are even more adversely affected than with W_3. The data shown in figure 11 for the other vertical-tail configurations also indicate similar effects of wing leading-edge variation on the aerodynamic characteristics.

The presence of the outboard vertical tails, V_{23}, at either the inboard or outboard location resulted in a loss of lift as illustrated in figure 12. Since these tails are located behind the moment reference the loss in lift also represents a loss in longitudinal stability. Similar results were obtained in the investigation reported in references 7 and 9.

The data of figure 13 show the effect of fuselage forebody strake, f_2, on the longitudinal characteristics; as would be expected, the effect on longitudinal stability is destabilizing. In the lower angle-of-attack range no significant effects of f_2 on the lift-drag characteristics are noted.

Lateral-Directional Characteristics

The effect of leading-edge profile on the lateral-stability parameters are shown in figure 14. The tests with leading edge, W_3, or $W_3 = 30^\circ$ indicated a significant reduction in C_{n_β} over much of the lift range as shown in figure 14. For W_3 the reduction was greatest at lowest lift coefficient decreasing to zero and becoming positive near a lift coefficient of 1.3. The losses sustained for leading edge, $W_3 = 30^\circ$, were generally much greater than that of W_3, particularly in the lower lift range.

It will be noted from figure 1 that a considerable part of the wing leading edge lies ahead of the moment reference, therefore, it would be expected that an increase in side area such as the addition of W_3 or $W_3 = 30^\circ$ would increase the side-force parameter $(-C_{Y_\beta})$. This characteristic contributes directly to instability as shown in figure 14(a). Not all of the negative effects arise directly from the leading edge. As indicated in figure 17, the vertical-tail contribution to stability, ΔC_{n_β}, shows that it is dependent upon the leading-edge contour and its location on the wing. The greatest contribution is obtained with leading edge W_1 and the least with $W_3 = 30^\circ$. It is probable that reduction in directional stability is associated with the modification of the leading-edge vortex. All contributions of V_{23} to stability are positive at the outboard wing location but at the inboard location (above the outboard nacelles) the contribution to stability is less and is negative above a lift coefficient of approximately 0.85. Somewhat similar results were obtained with the centerline vertical tail, V_6.

The results of tests with the centerline fin, V_4 , and forebody strake, f_2 , are shown in figure 16. The centerline fin, V_4 , shows as does ventral fin, V_6 , positive increments in C_{n_β} for a limited lift coefficient range. The loss in directional stability probably results from the movement of the vertical tail out of the favorable sidewash field as would be indicated by the variation of C_{Y_β} with C_L . Use of the forebody strake, f_2 , gives positive increments in C_{Y_β} and provides directional stability throughout the lift range. Tests of V_4 and f_2 in combination show positive values of C_{n_β} to a lift coefficient of 1.35. It will be noted that the algebraic sum of the separate values from the strake, f_2 , and fin, V_4 , are approximately equal to C_{n_β} obtained from tests of the combination.

Effective dihedral.- Because of the high leading-edge sweep all configurations investigated showed relative large values of the effective dihedral parameter, C_{ℓ_β} , in the range of lift coefficients from 0.5 to 0.6 (see figures 14 to 16). The modified leading edges, W_3 and $W_3 = 30^\circ$ when used alone or in combination with a centerline tail resulted in a loss of C_{ℓ_β} above lift coefficients of 0.6 as shown in figures 14(a) and 14(b). The presence of the outboard vertical tail, $V_{23,0}$, had a major effect on C_{ℓ_β} in that it tended to nullify the effects of the individual leading-edge configuration. Both vertical-tail configuration, $V_{23,0}$ and V_4 , in combination with wing, W_1 , tended to reduce C_{ℓ_β} in the low-lift range, a desirable characteristic when landing in a strong crosswind.

CONCLUSION

A low-speed investigation has been made on a highly-swept wing model to determine the effects of wing leading edge and vertical-tail configuration on the characteristics in pitch and sideslip. The tests were made with trailing-edge flaps deflected over an angle-of-attack range from 8° to 32°. The results are summarized as follows:

The basic wing configuration had a pitch-up tendency that began at about 11°, a modification to the wing which increased the leading-edge radius, extended the angle for pitchup to about 19°, and use of a leading-edge flap practically eliminated the pitch-up tendency. The modified leading edges resulted in favorable increases in lift-drag ratio and undesirable increases in the angle of attack and pitching-moment coefficient for a given lift coefficient. The presence of the outboard vertical tails caused a loss of lift which was destabilizing in pitch, but use of the vertical tails with the basic wing provided good directional stability. The thickened leading edge reduced the directional stability for all vertical-tail configurations and the directional stability was decreased even more by deflection of the leading edge.

Positioning the outboard vertical tails above engine nacelles reduced both the longitudinal and directional stability. A forebody strake in combination with a relatively small centerline vertical tail provided directional stability to a lift coefficient of 1.35.

The modified leading edges caused large reductions in dihedral effect with the outboard vertical tails off above lift coefficients of 0.6, however, with the vertical tails on there was little difference in dihedral effect.

REFERENCES

1. Morris, Odell A.; and Fournier, Roger H.: Aerodynamic Characteristics at Mach Numbers 2.30, 2.60, and 2.96 of a Supersonic Transport Model Having a Fixed, Warped Wing. NASA TM X-1115, 1965.

2. Morris, Odell A.; and Patterson, James C., Jr.: Transonic Aerodynamic Characteristics of Supersonic Transport Model With a Fixed, Warped Wing Having 74° Sweep. NASA TM X-1167, 1965.

3. Henderson, William P.: Low-Speed Aerodynamic Characteristics of a Supersonic Transport Model With a Highly Swept, Twisted and Cambered Fixed Wing. NASA TM X-1249, July 1966.

4. Ray, Edward J.; and Henderson, William P.: Low-Speed Aerodynamic Characteristics of a Highly Swept, Supersonic Transport Model With Auxiliary Canard and High-Lift Devices. NASA TM X-1694, 1968.

5. Lockwood, Vernard E.; and Huffman, Jarrett K.: The Aerodynamic Characteristics of a Fixed Arrow Wing Supersonic Transport Configuration (SCAT 15F-9898). Part I - Stability and Performance Characteristics in the Landing and Take-Off Configuration. NASA LWP-766, June 1969.

6. Lockwood, Vernard E.: The Aerodynamic Characteristics of a Fixed Arrow Wing Supersonic Transport Configuration (SCAT 15F-9898). Part IA - Additional Studies of the Stability and Performance Characteristics in the Landing and Take-Off Configuration. NASA LWP-842, January 1970.

7. Lockwood, Vernard E.; and Driver, Cornelius: The Aerodynamic Characteristics of a Fixed Arrow Wing Supersonic Transport Configuration (SCAT 15F-9898). Part IB - Studies of the Low-Speed Stability and Performance Characteristics to 35° Angle of Attack. NASA LWP-899, September 1970.

8. Lockwood, Vernard E.; and Huffman, Jarrett K.: The Aerodynamic Characteristics of a Fixed Arrow Wing Supersonic Transport Configuration (SCAT 15F-9898). Part IV - Aerodynamic Characteristics in Ground Effect. NASA LWP-828, November 1969.

9. Freeman, Delma C., Jr.: Low-Subsonic Longitudinal Aerodynamic Characteristics in the Deep-Stall Angle-of-Attack Range of a Supersonic Transport Configuration With a Highly Swept Arrow Wing. NASA TM X-2316, September 1971.

10. Re, Richard J.; and Couch, Lana M.: The Aerodynamic Characteristics of a Fixed Arrow Wing Supersonic Transport Configuration (SCAT 15F-9898). Part III - Reynolds Number Effects on the Stability Characteristics in the Deep Stall Angle-of-Attack Range. NASA LWP-735, April 1969.

11. Gillis, Clarence L., Polhamus, Edward C., and Gray, Joseph L., Jr.: Charts for Determining Jet-Boundary Corrections for Complete Models in the 7- by 10-Foot Closed Rectangular Wind Tunnels. NACA WR L-123, 1945.

12. Herriot, John G.: Blockage Corrections for Three-Dimensional Flow Closed-Throat Wind Tunnel, With Consideration of the Effect of Compressibility. NACA Rept. 995.

TABLE I - DIMENSIONAL CHARACTERISTICS OF MODEL

Wing (Reference Dimensions)	
Area, sq ft	8.908
Span, ft	3.804
Chord, ft	3.192
Aspect ratio	1.624
Sweep of leading edge	
Main wing, deg	74
Tip, deg	65
(Actual Dimensions)	
Area, sq ft	10.160
Span, ft	4.133
Chord, ft	3.456
Aspect ratio	1.682
Sweep of leading edge	
Main wing, deg	74
Center, deg	70.5
Tip, deg	60.0
Fuselage	
Length, ft (nose undeflected)	9.000
Nacelle, E_2	
Length, ft	1.121
Inside diameter, ft	0.155
Outside diameter, ft	0.203
Horizontal Tail, H_4	
Root chord, ft	0.853
Tip chord, ft	0.310
Span, ft (panel)	0.372
Area, sq ft (panel)	0.190
Leading-edge sweep, deg	60.0
Trailing-edge sweep, deg	- 2.0
Dihedral angle, deg	-15.0
Incidence angle, deg	0

TABLE I - CONTINUED

Vertical Tails ($V_{23,I}$ and $V_{23,O}$)	
V_{23}	
Area, sq ft (each)	0.219
Root chord, ft (approximate)	1.28
Tip chord, ft	0.17
Span, ft (approximate)	0.335
Sweep of the leading edge, deg	74.5
Sweep of the trailing edge, deg	17.2
V_4	
Area, sq ft	0.190
Span, ft	0.408
Root chord, ft	0.78
Tip chord, ft	0.150
Sweep of leading edge, deg	52
Sweep of trailing edge, deg	14.9
V_6	
Rudder area, sq ft	0.0986
Ventral fin area, sq ft	0.1910

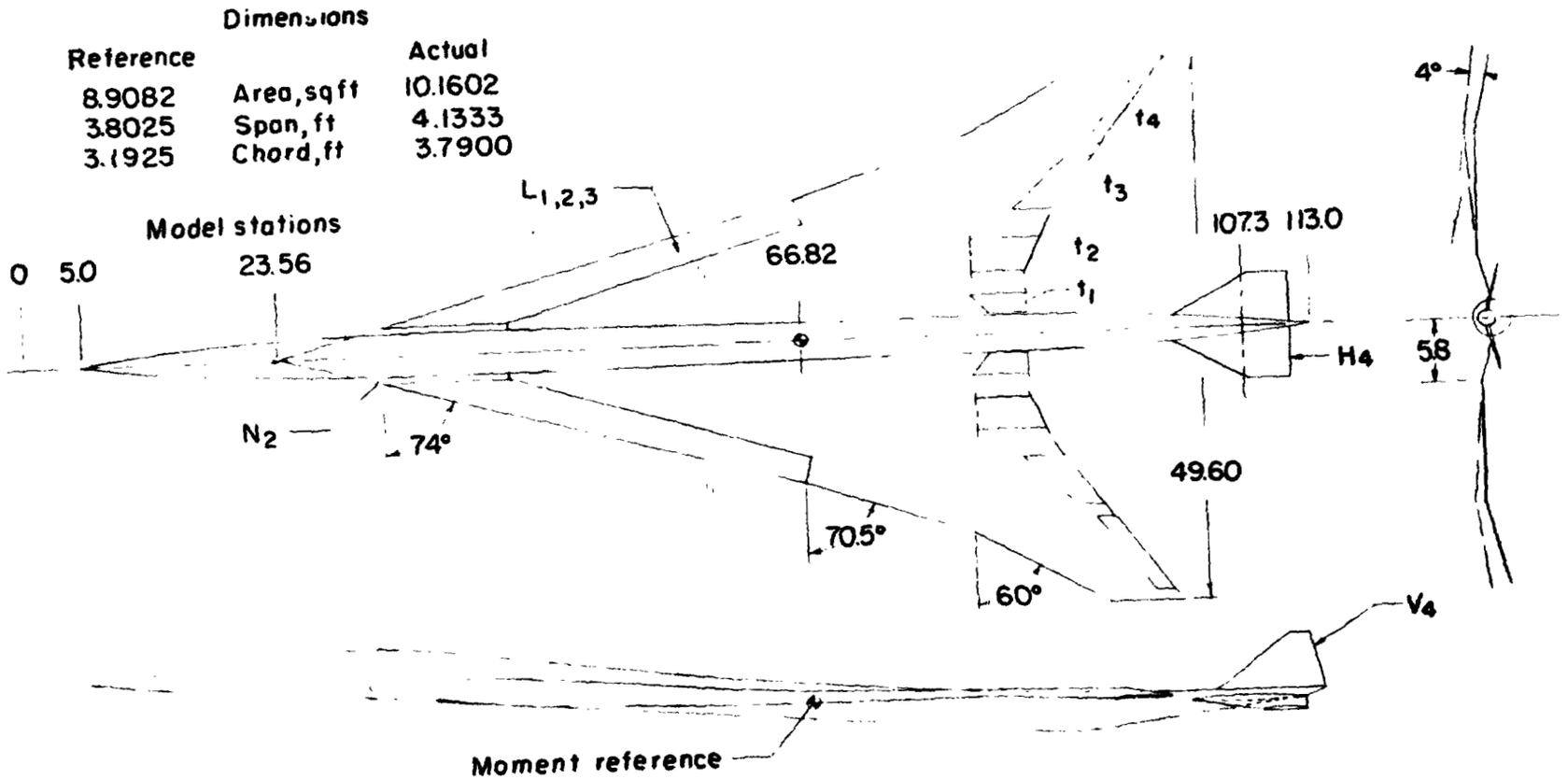

Figure 1.- Three-view drawing of the model.

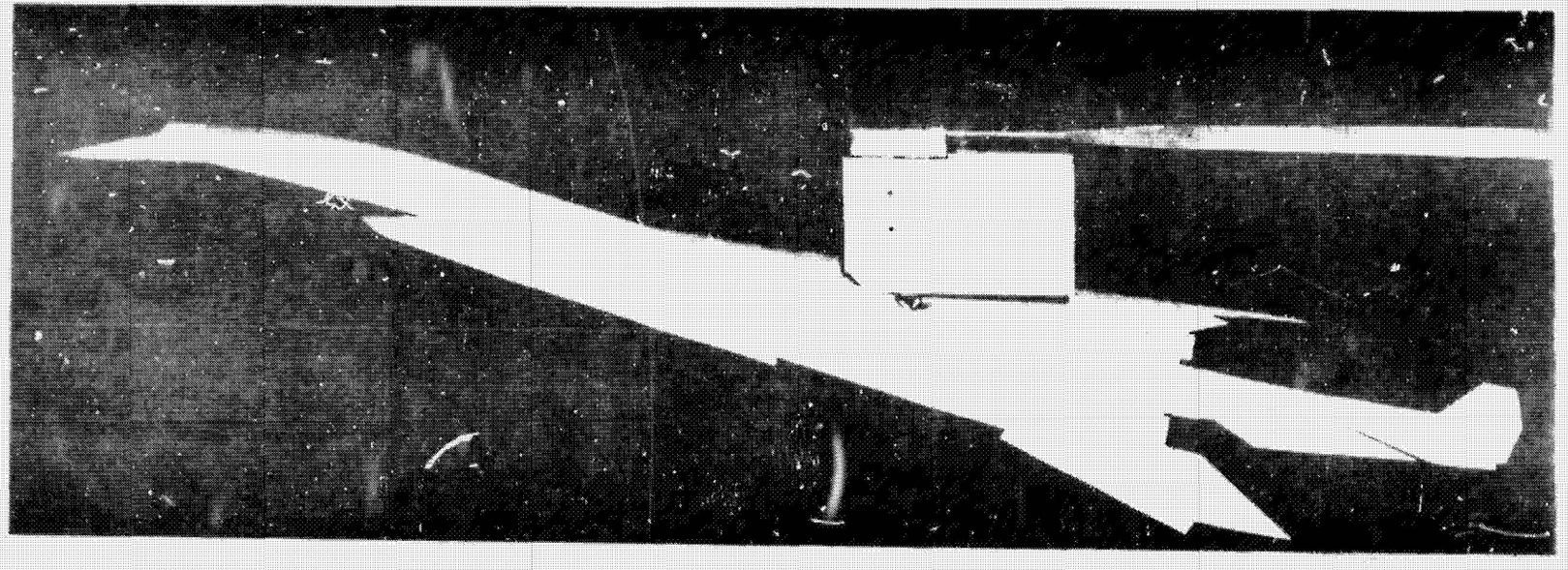

Figure 2.- Photograph of model configuration, $B_9N_2W_2(L_{1-3} = 30^0)E_2H_4$, with overhead sting support.

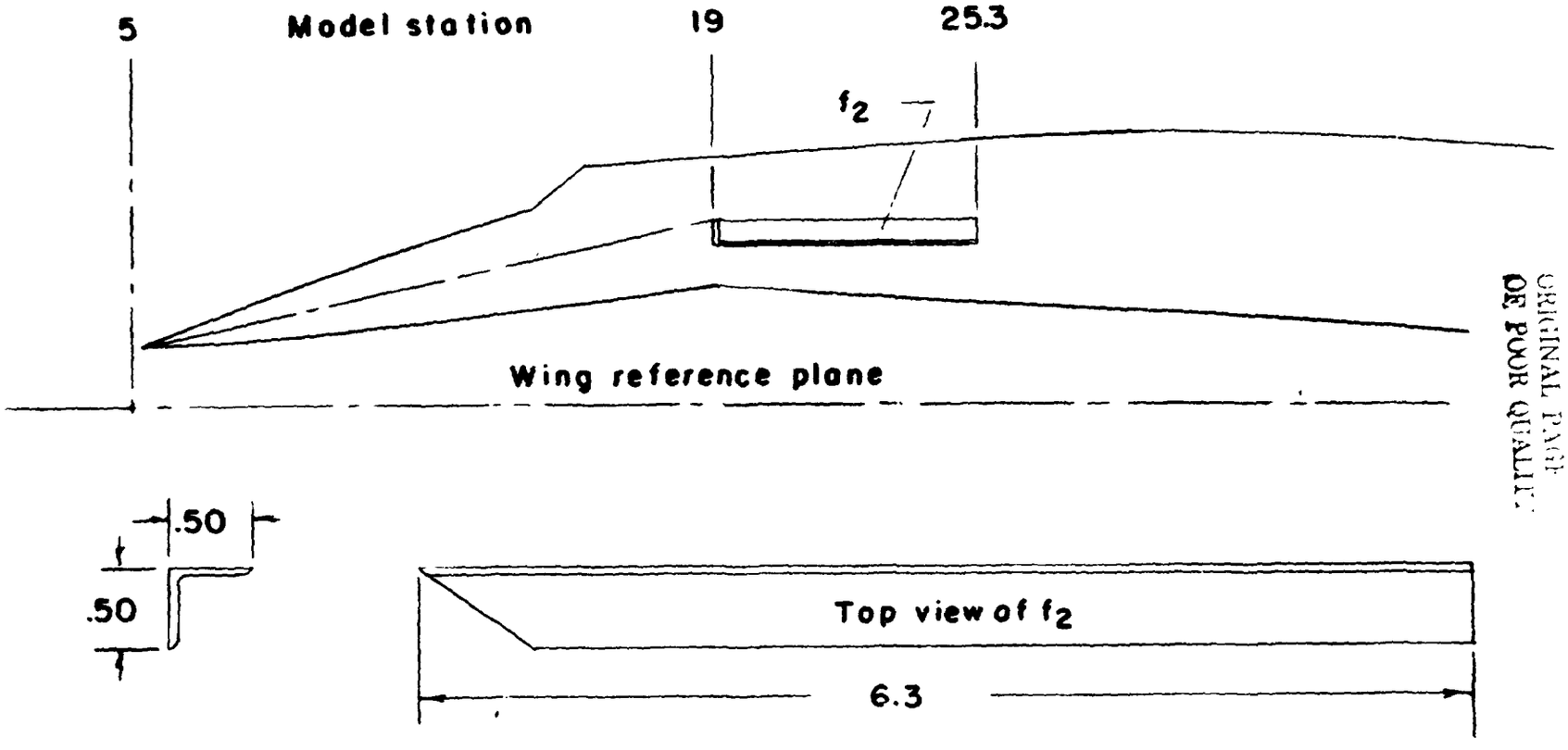

Figure 3.- Drawing of the deflected fuselage nose with the strake, f_2, used in some tests.

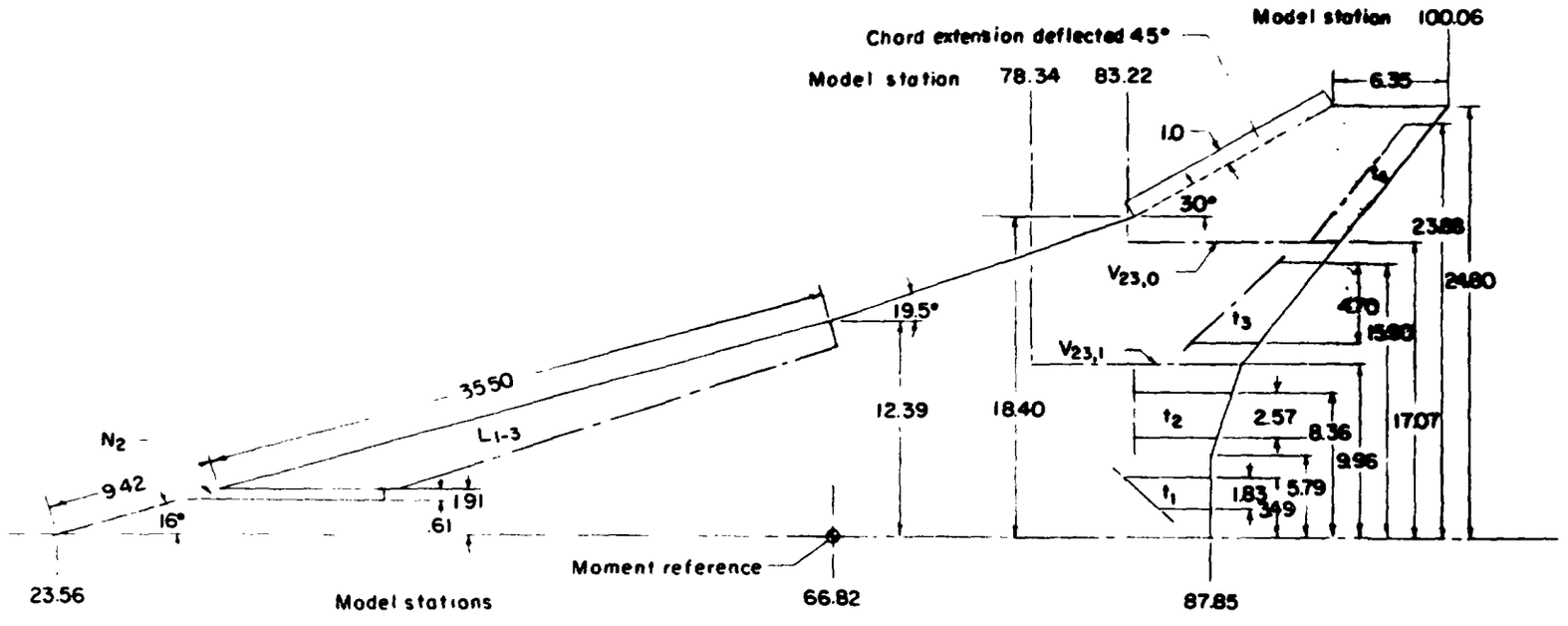

Figure 4.- Drawing of the leading- and trailing-edge flap system.

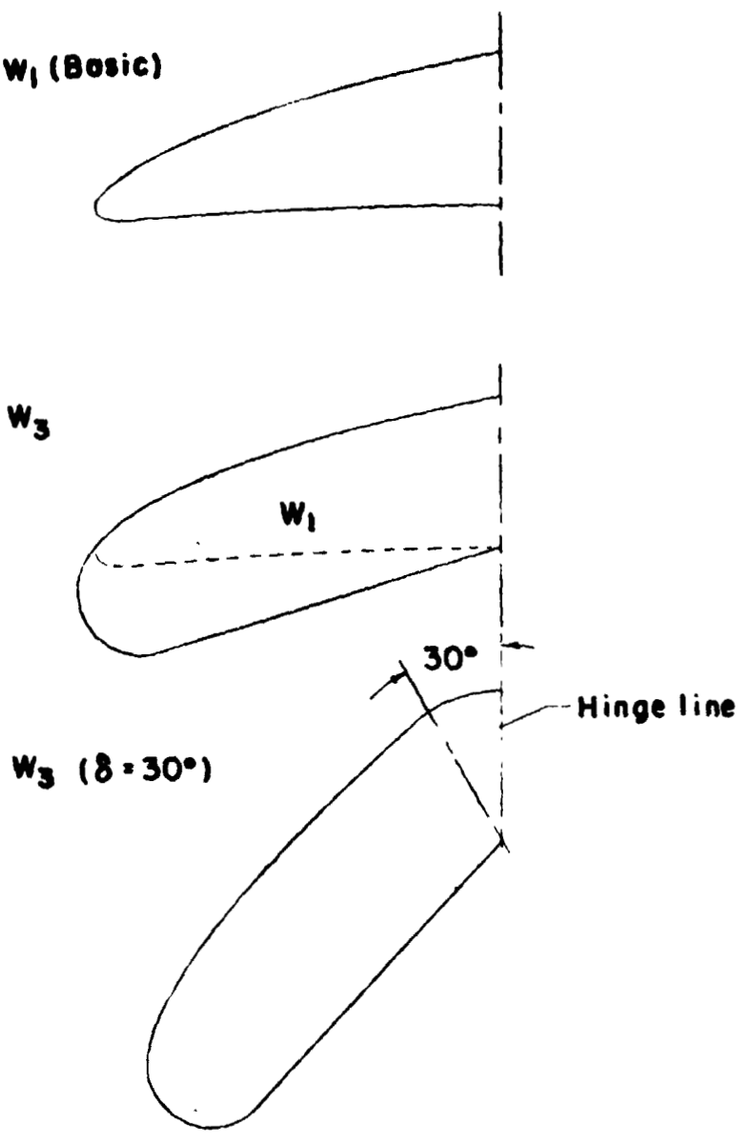

Figure 5.- Typical profiles of the leading-edge flaps. L_{1-3}.

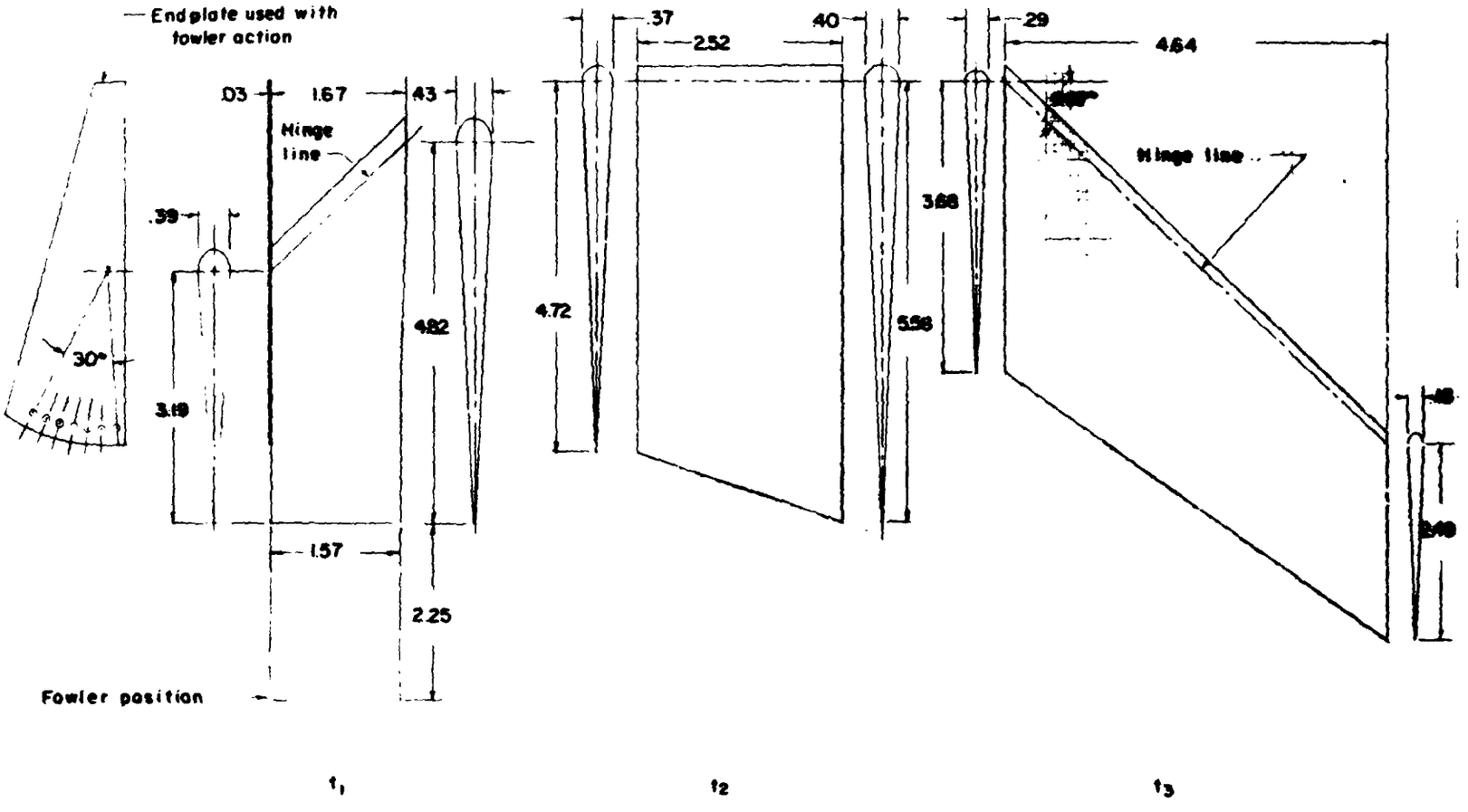

Figure 6.- Details of the trailing-edge flaps, t_1, t_2, and t_3.

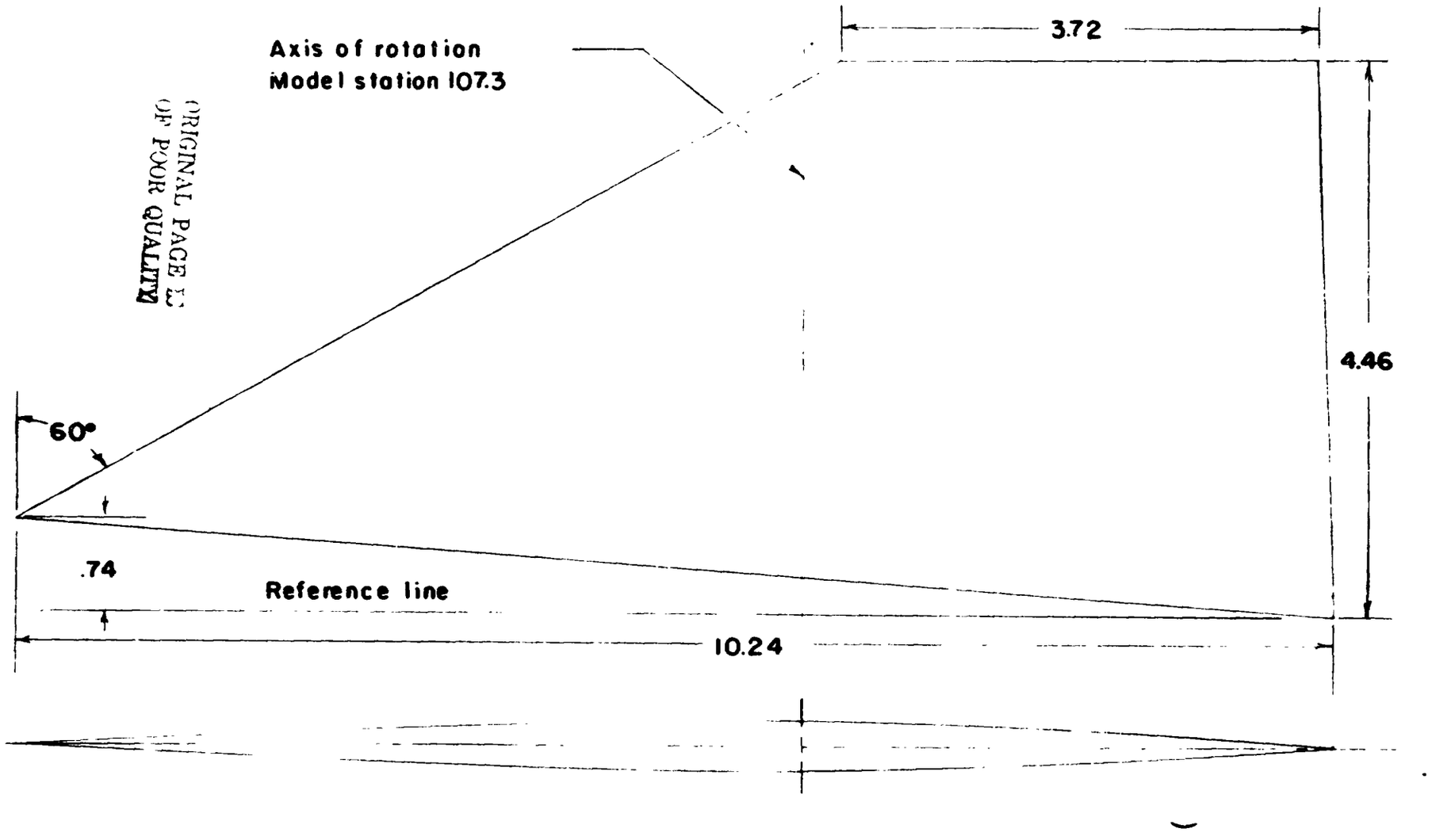

Figure 7.- Drawing of the horizontal tail, H_4.

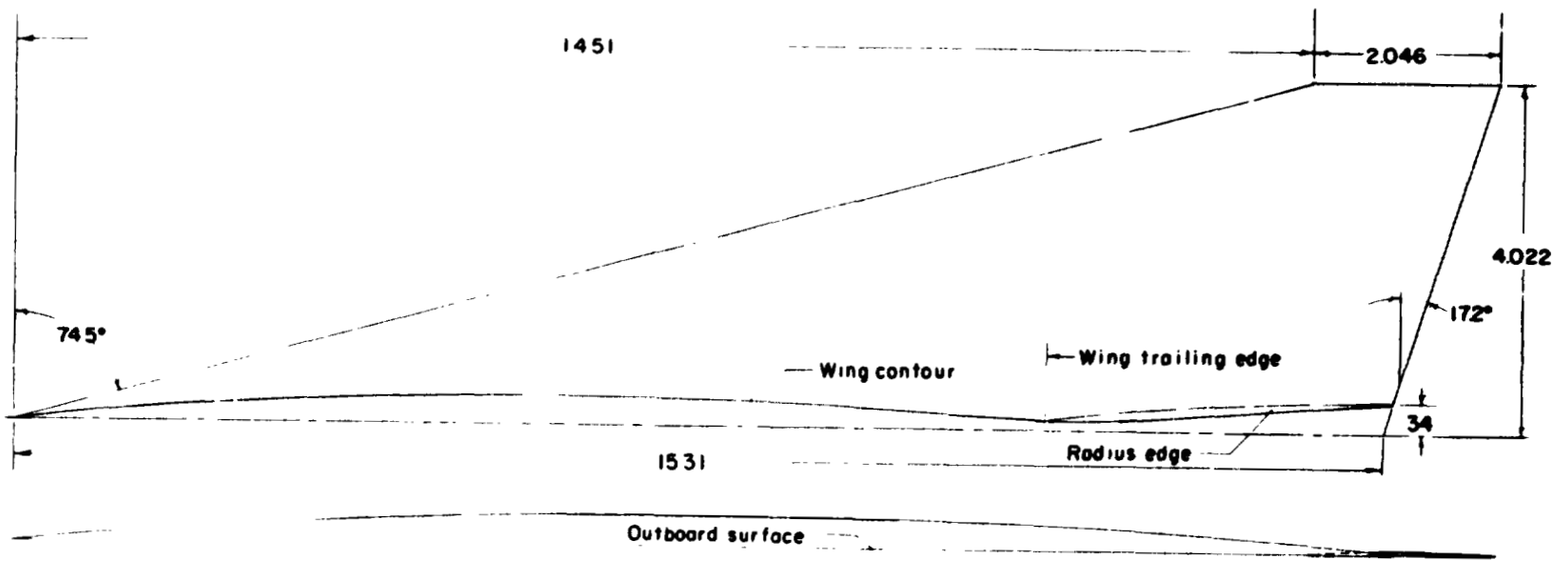

(a) V_{23}

Figure 8.- Drawing of the vertical tails.

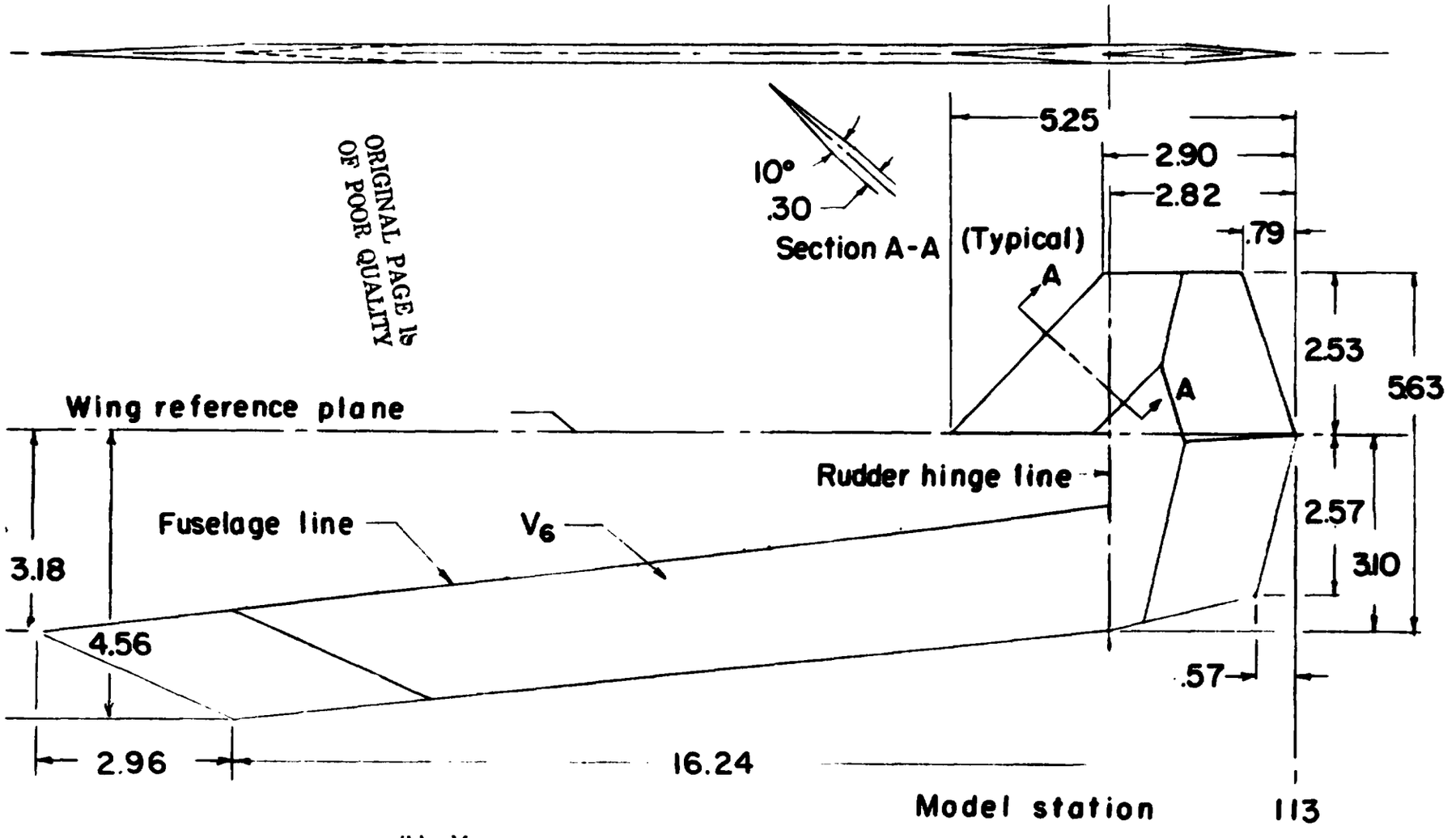

(b) V_6

Figure 8.- Continued.

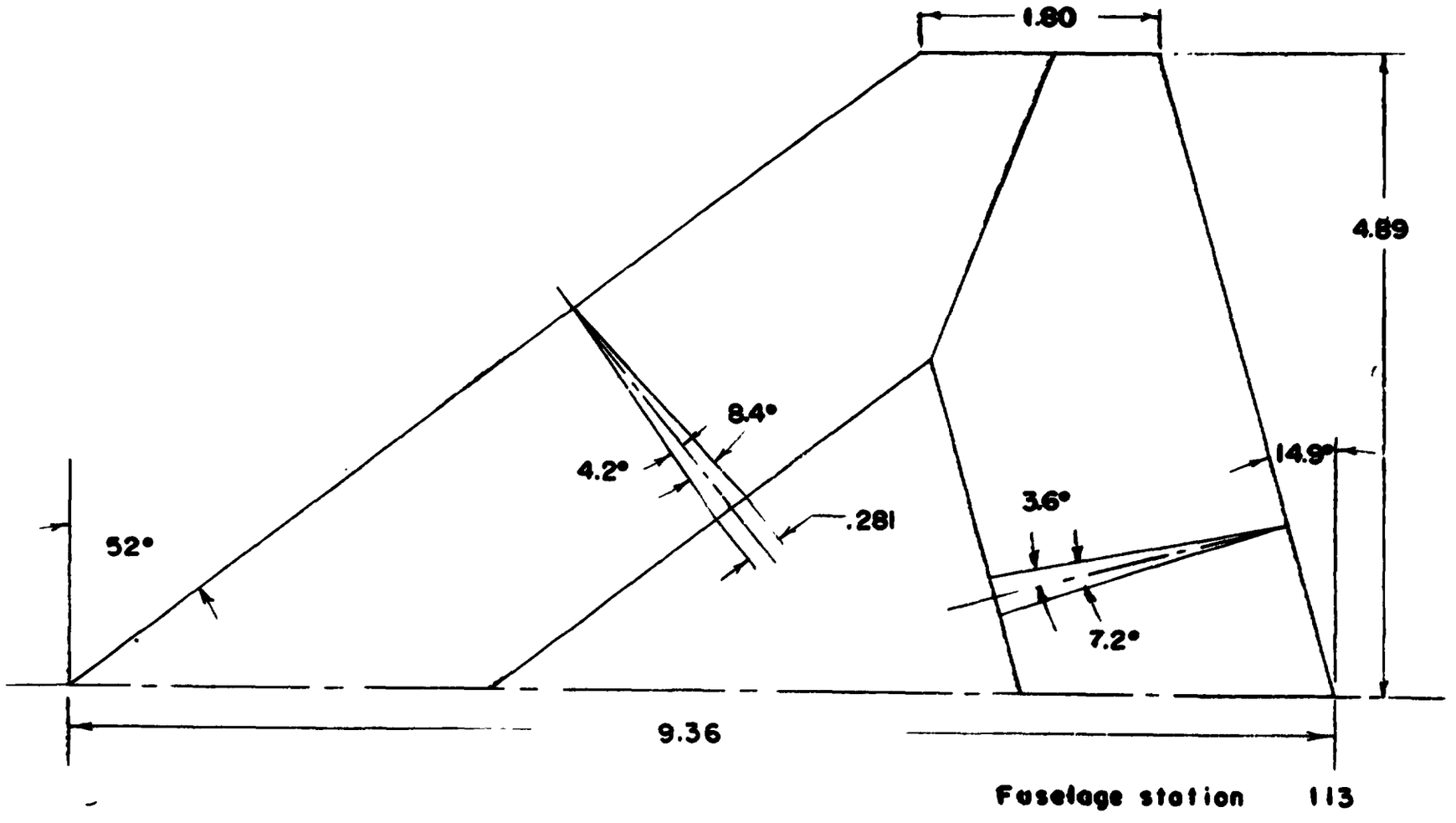

(c) V_4

Figure 8.- Concluded.

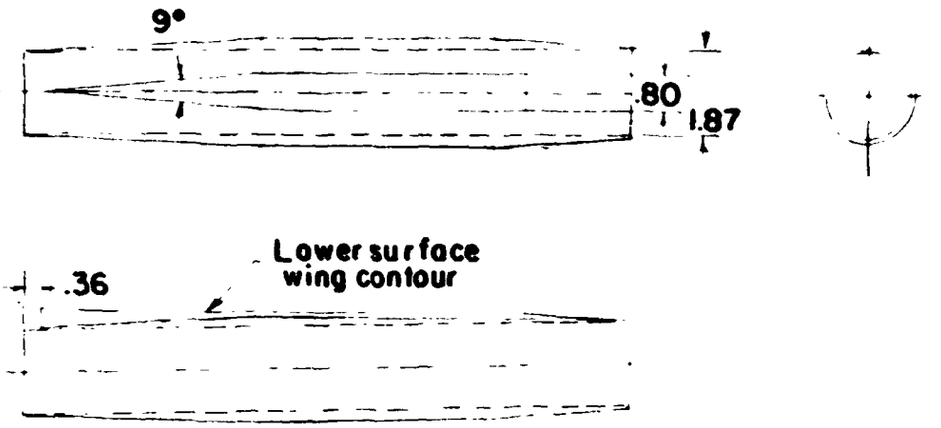

Outboard engine nacelle
(Spanwise station 9.96)

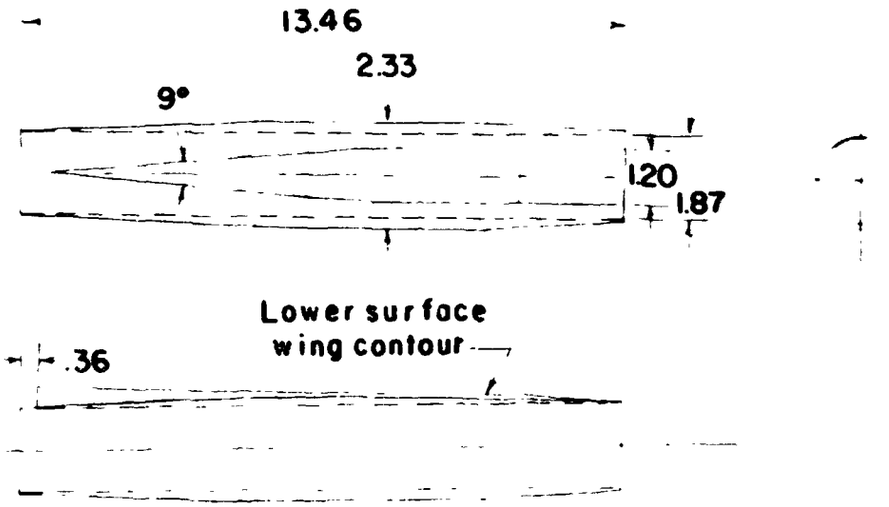

Inboard engine nacelle
(Spanwise station 4.74)

Figure 9.- Drawing of the inboard and outboard engine nacelles, E_2.

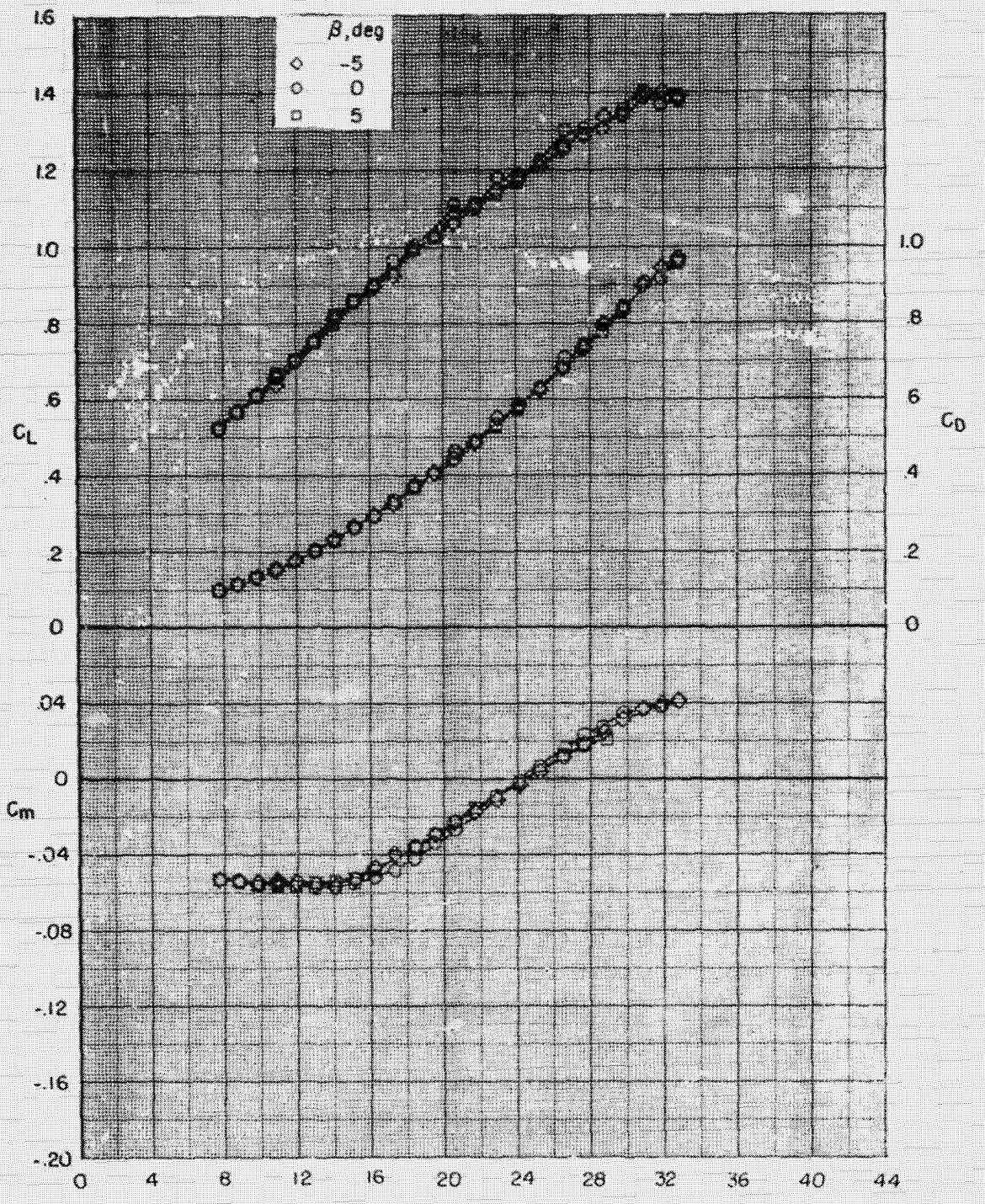

Figure 18.- Effect of sideslip angle on the longitudinal characteristics.
$W_1 = 0^0$; V_6 V_{230}

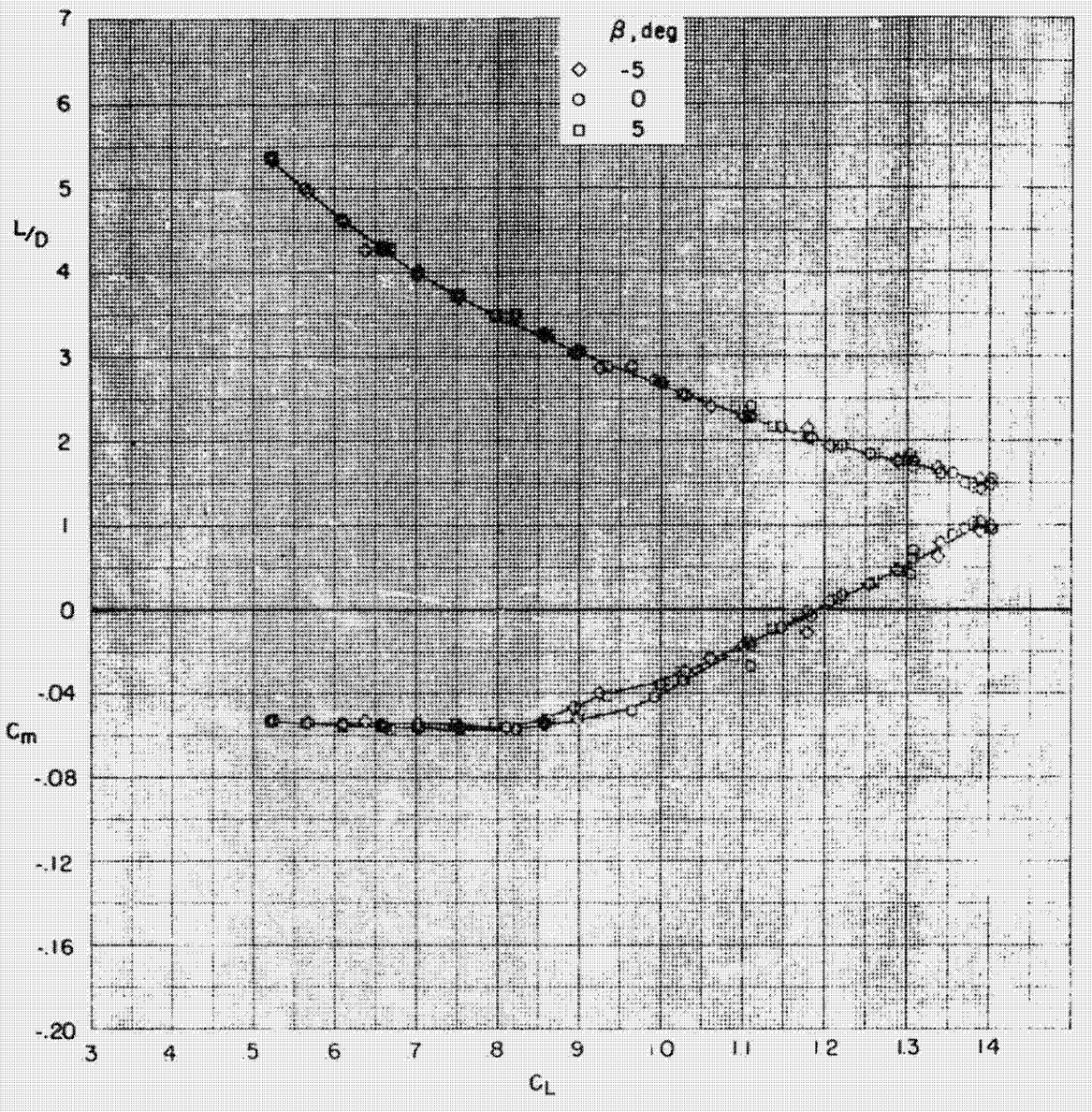

Figure 10.- Concluded.

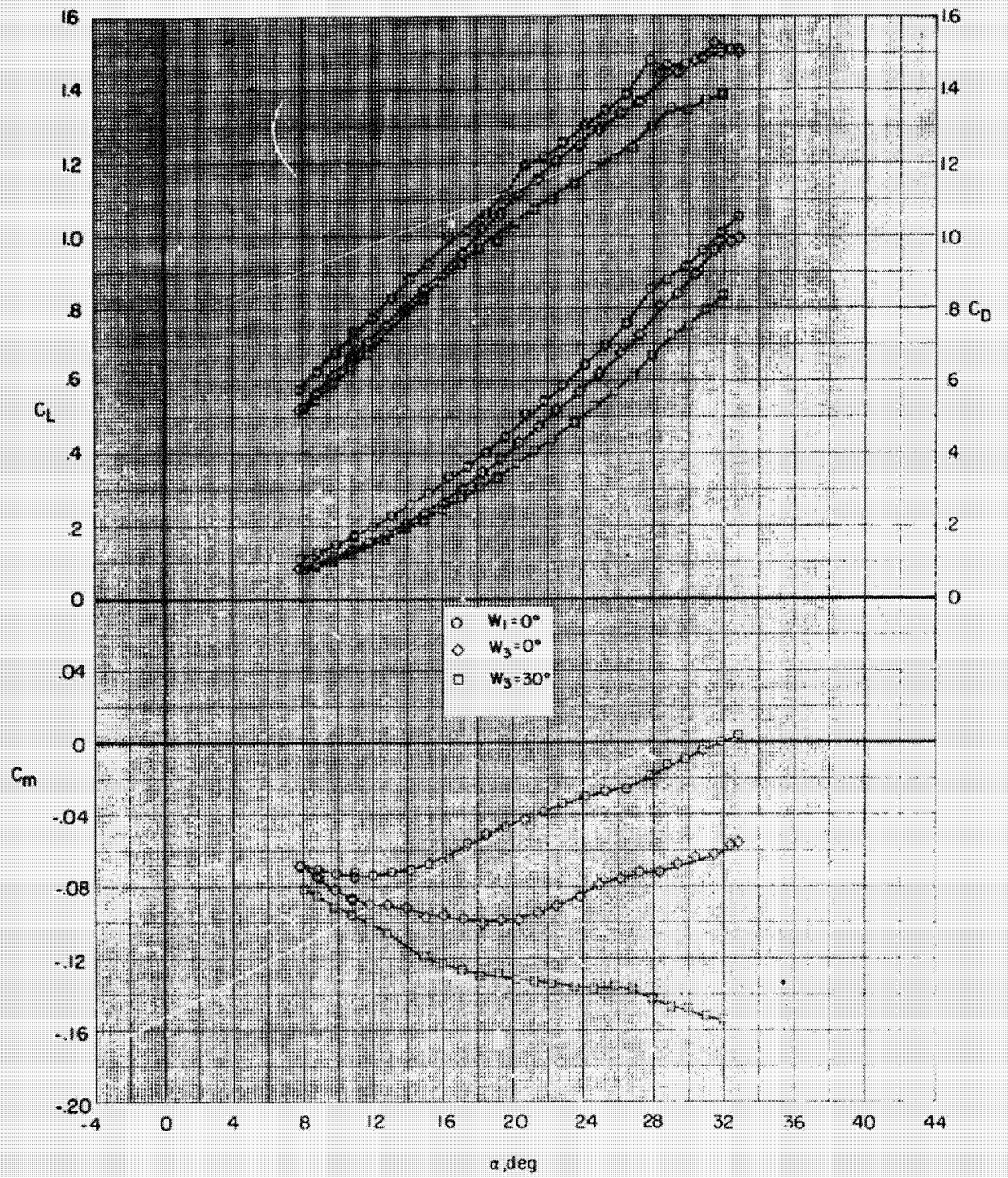

(a) V_{Off}

Figure 11.- Effect of wing leading edge configuration on the longitudinal characteristics, β -5°

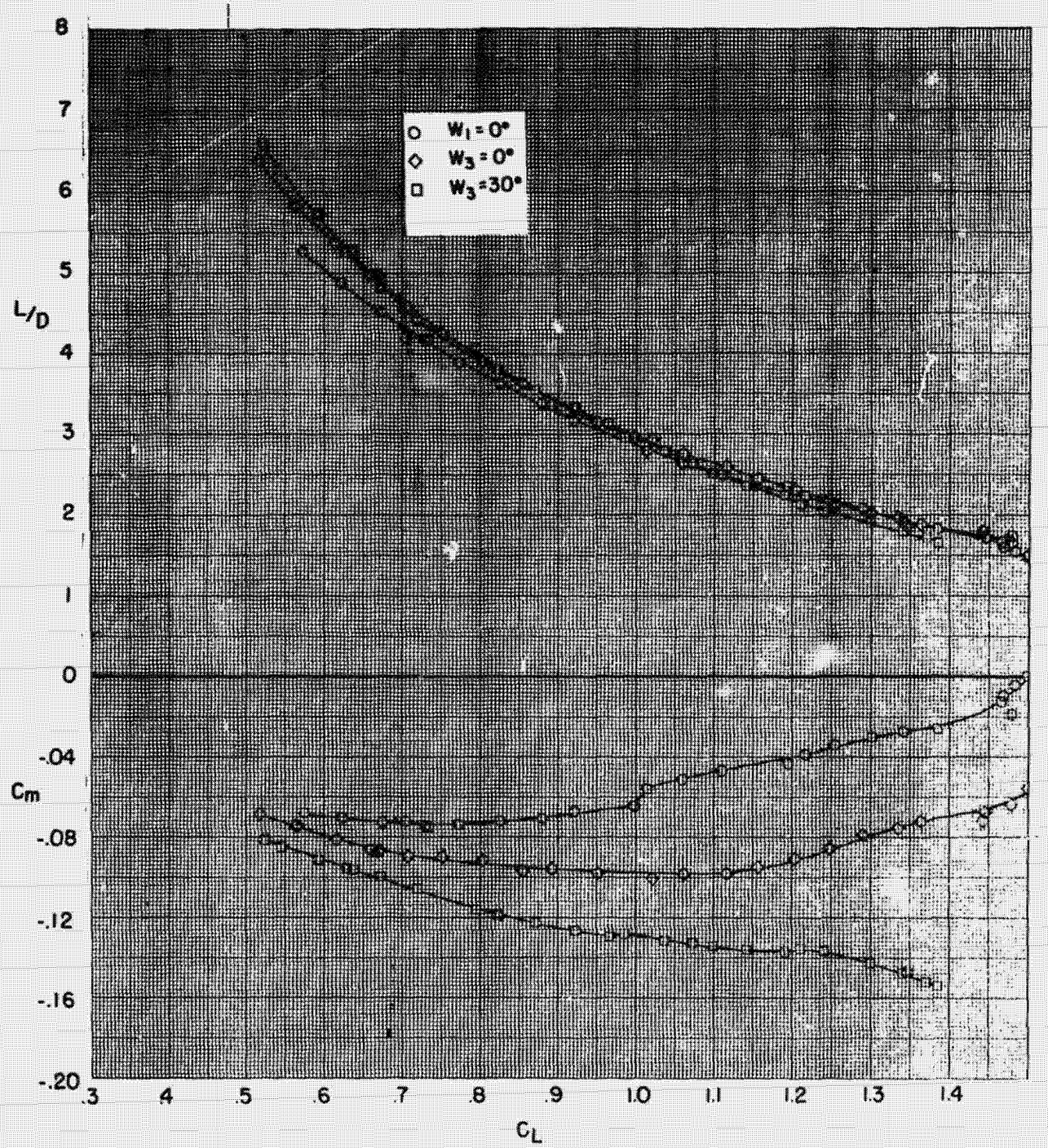

(a) Concluded.
Figure 11.- Continued.

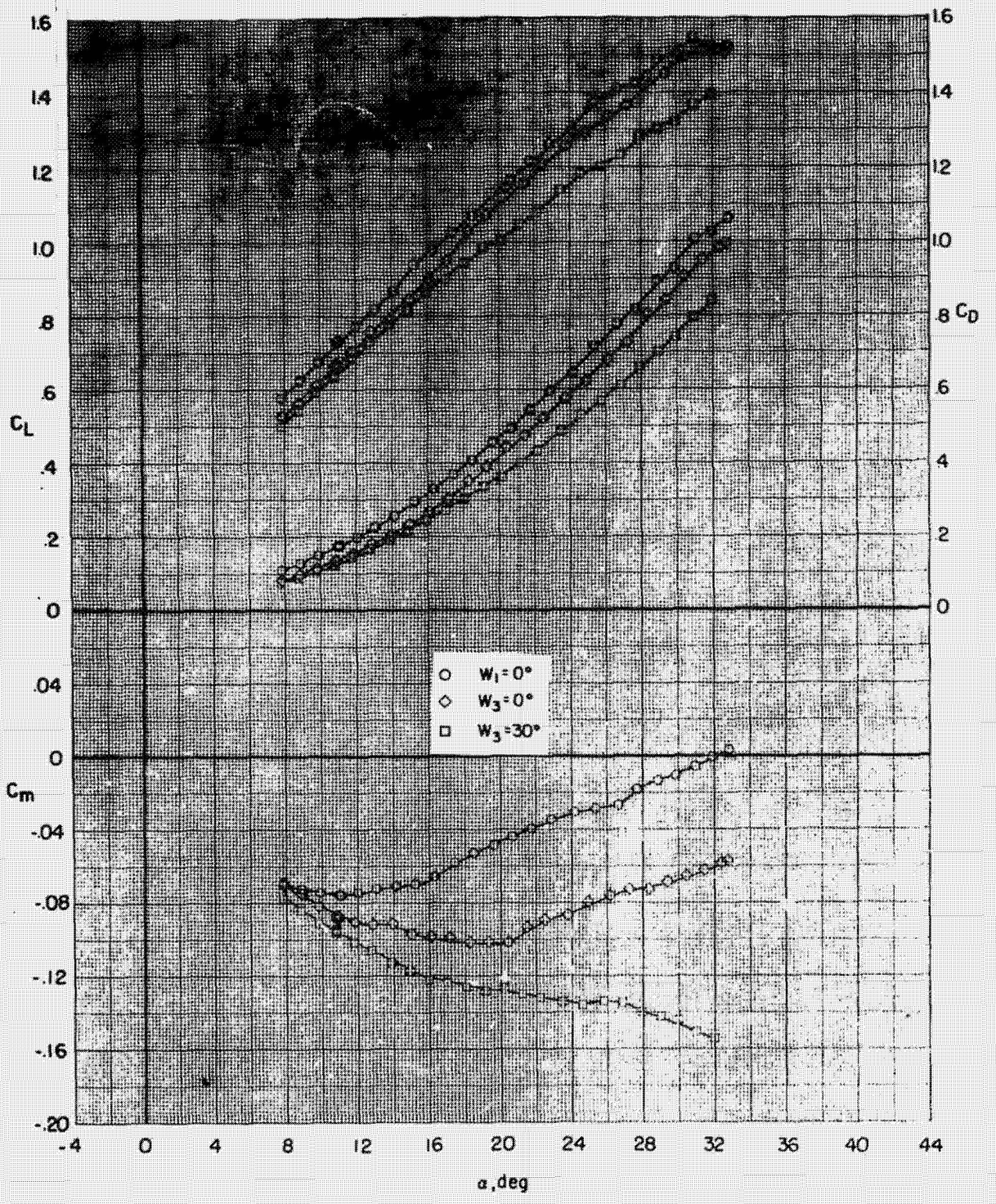

(b) V_6
Figure 11.- Continued.

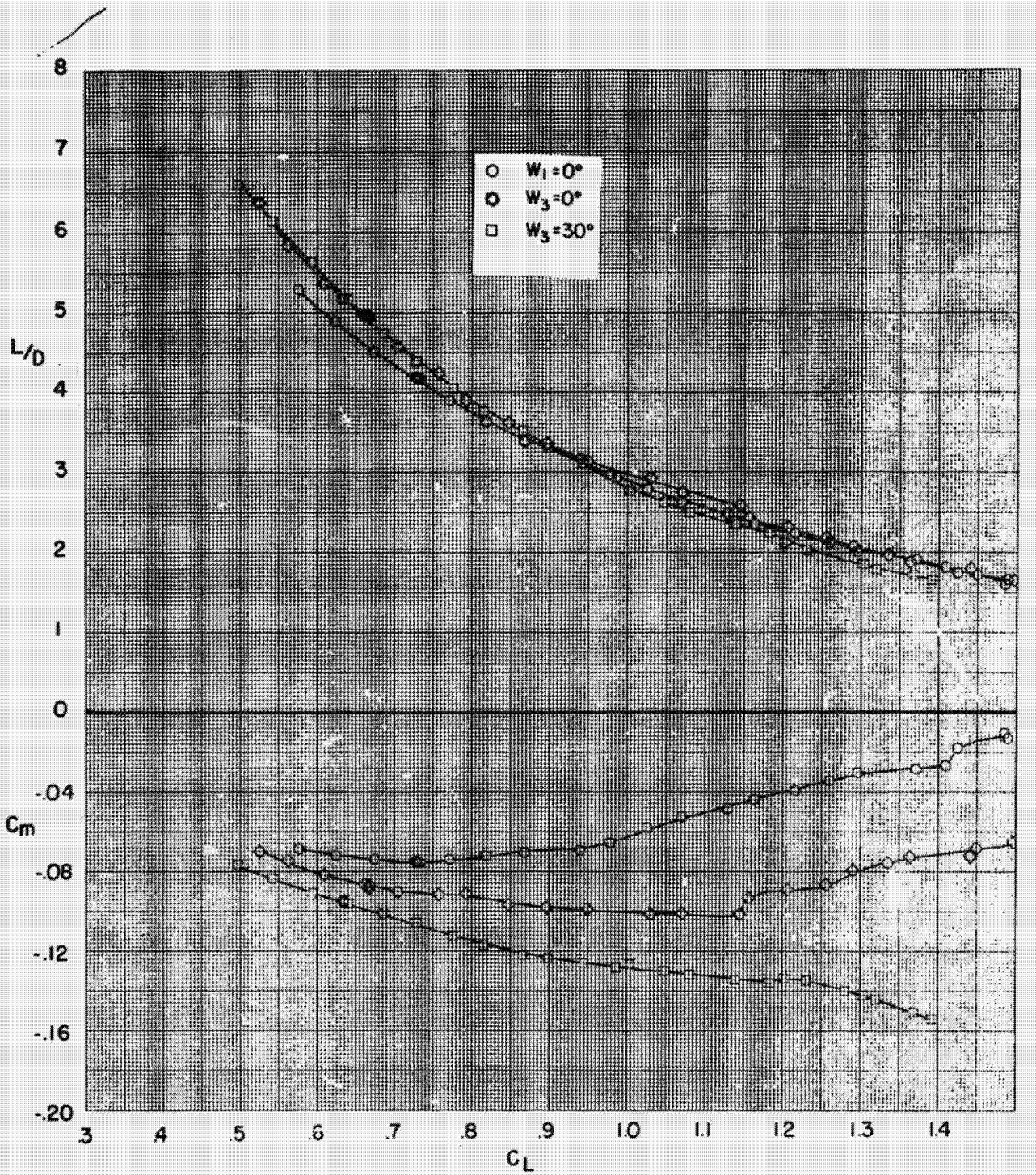

(b) Concluded
Figure 11.- Continued.

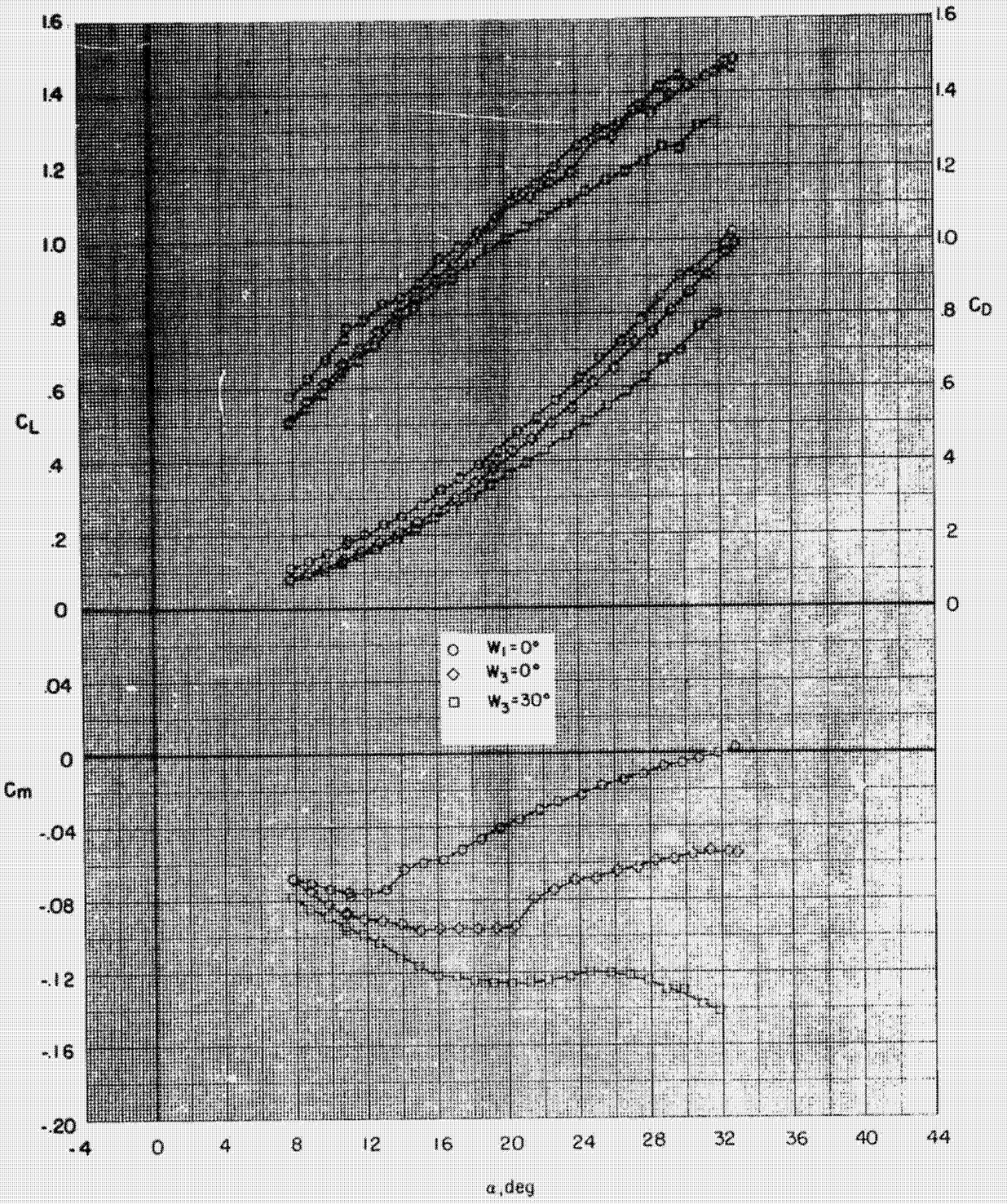

(c) V_6, V_{23} (I)
Figure 11.- Continued.

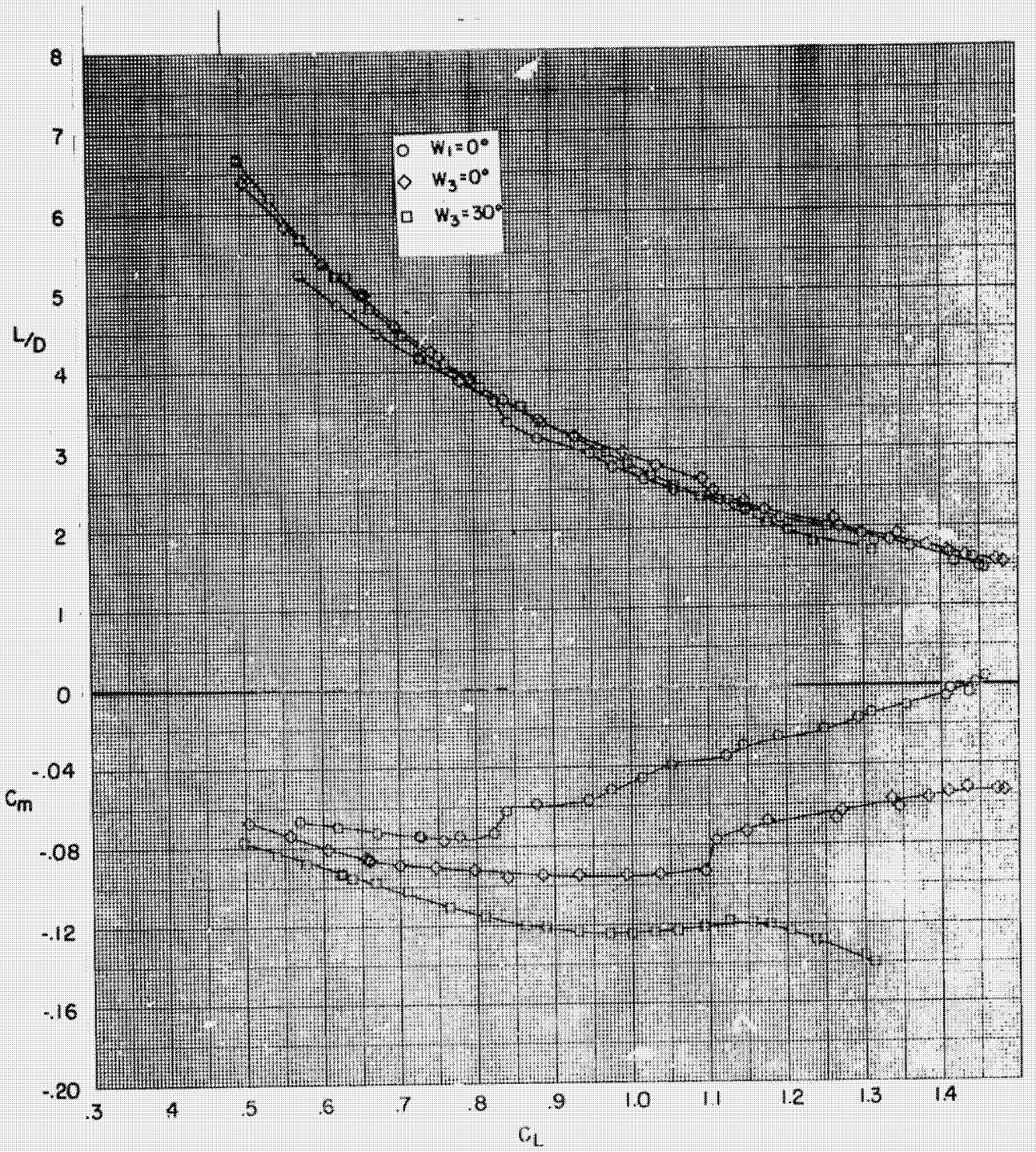

(c) Concluded.
Figure 11.- Continued.

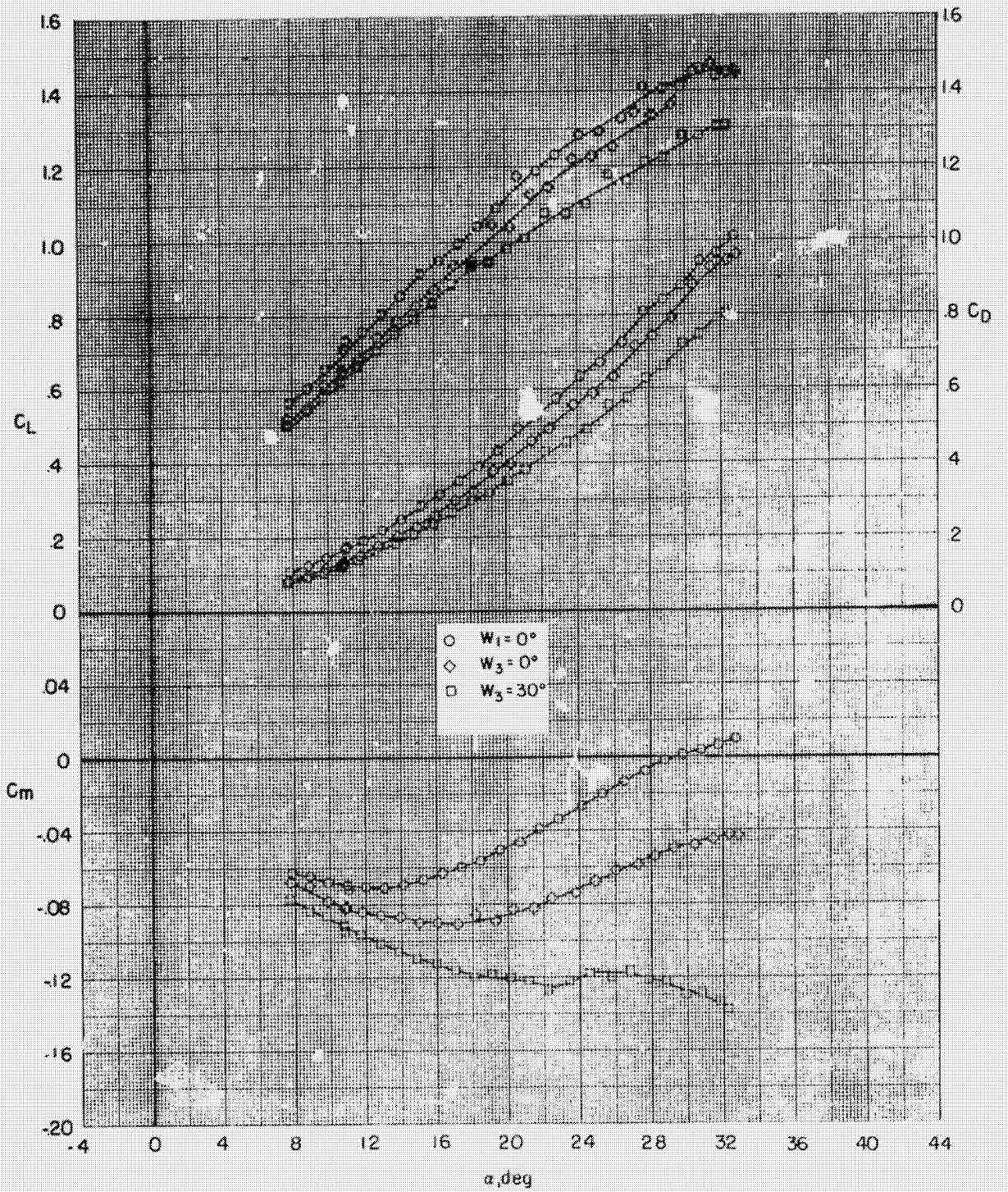

(d) V_6, V_{23} (0)
Figure 11.- Continued

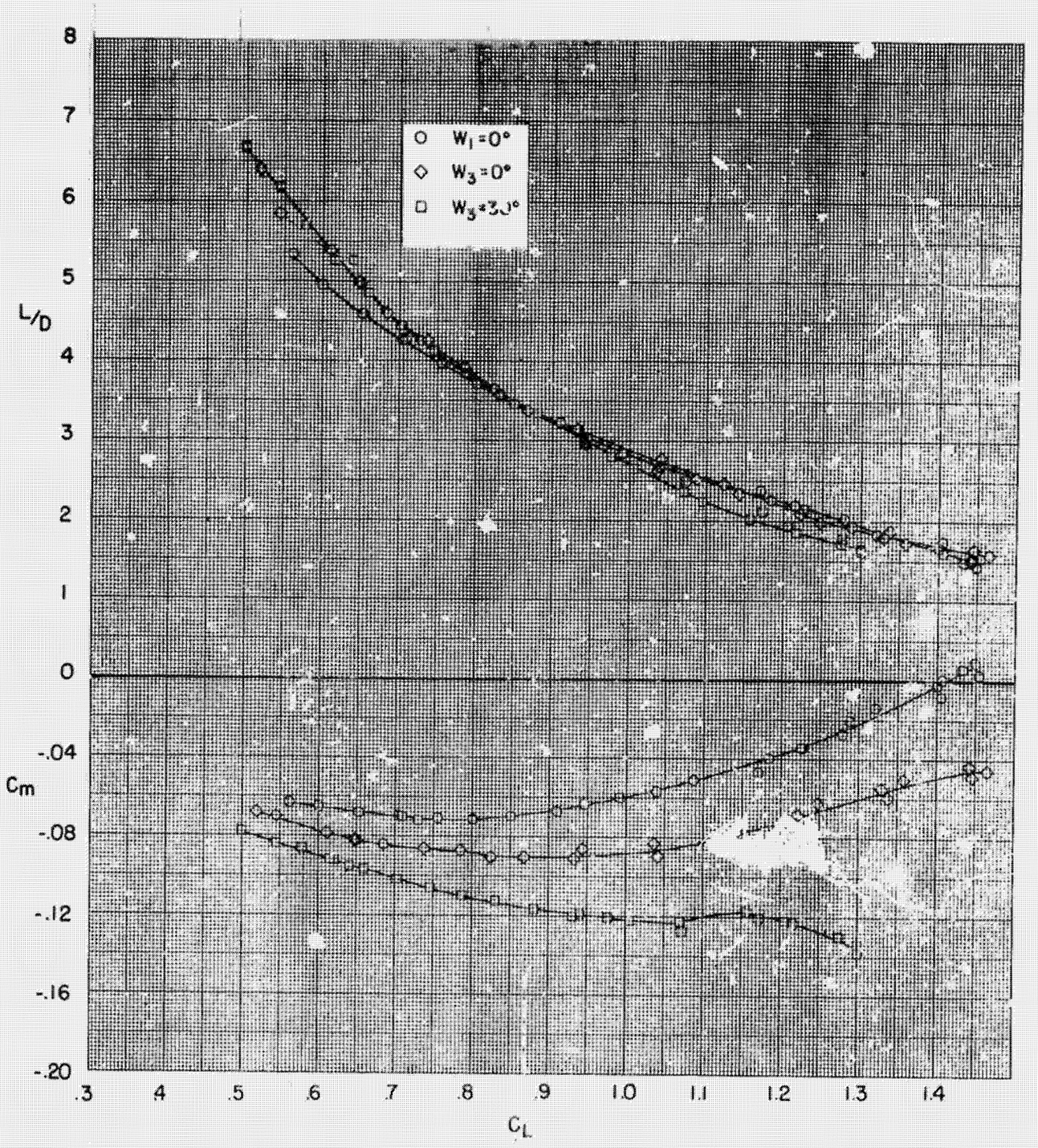

(d) Concluded.

Figure 11.-Concluded.

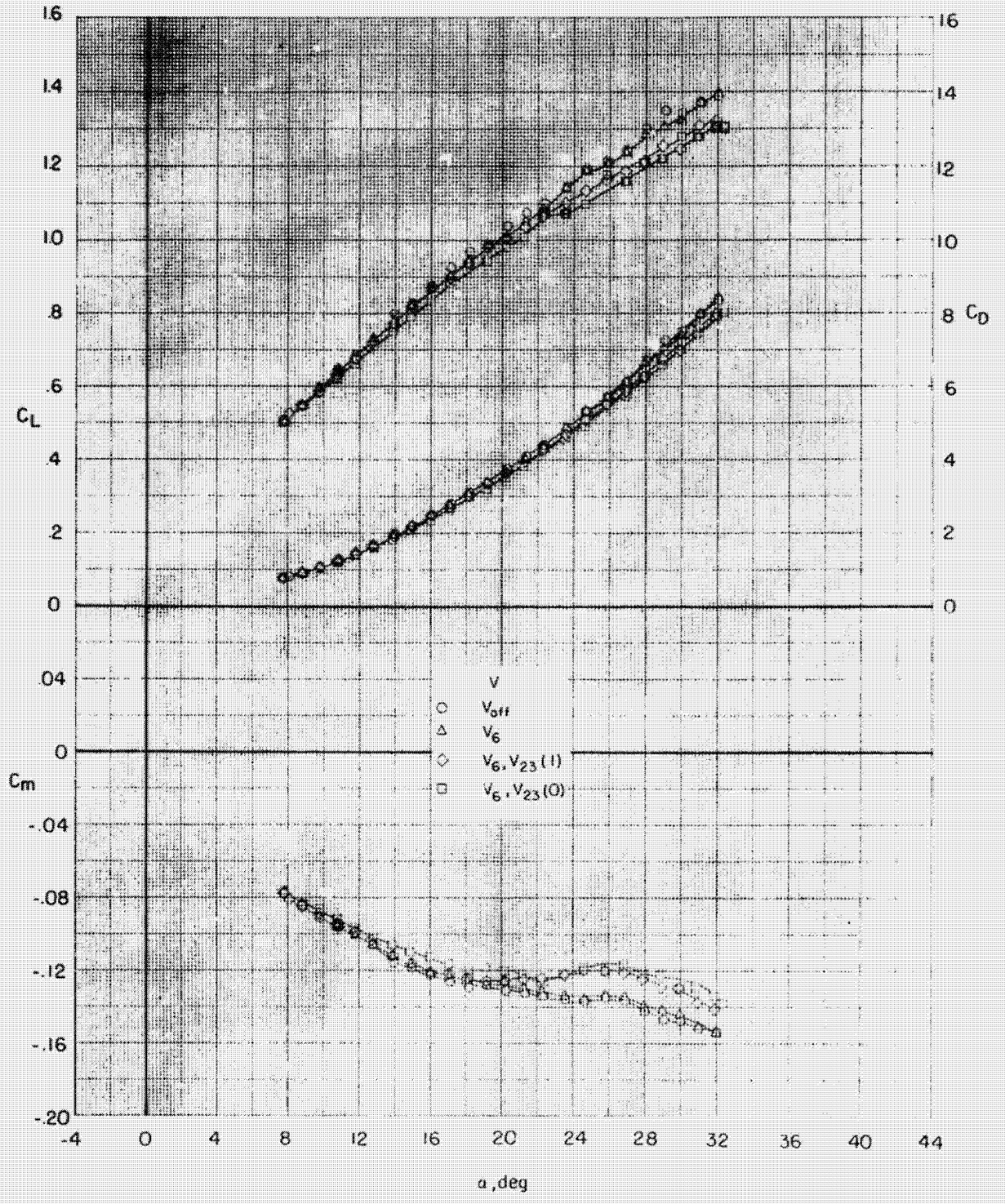

(a) $W_3 = 30^0$

Figure 12.- Effect of vertical tail configuration on the longitudinal characteristics. $\beta = 0$

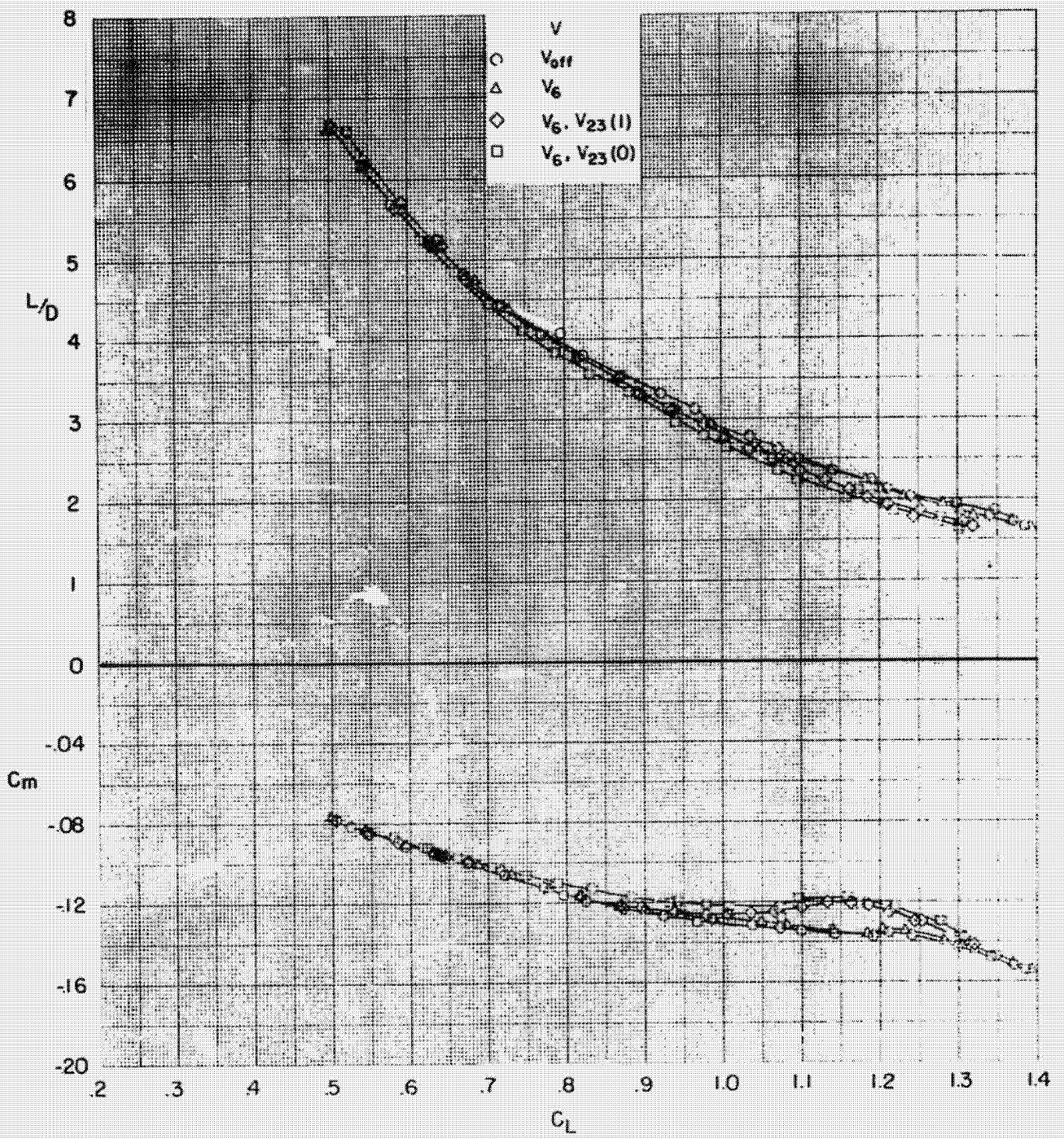

(a) Concluded.
Figure 12 .- Continued.

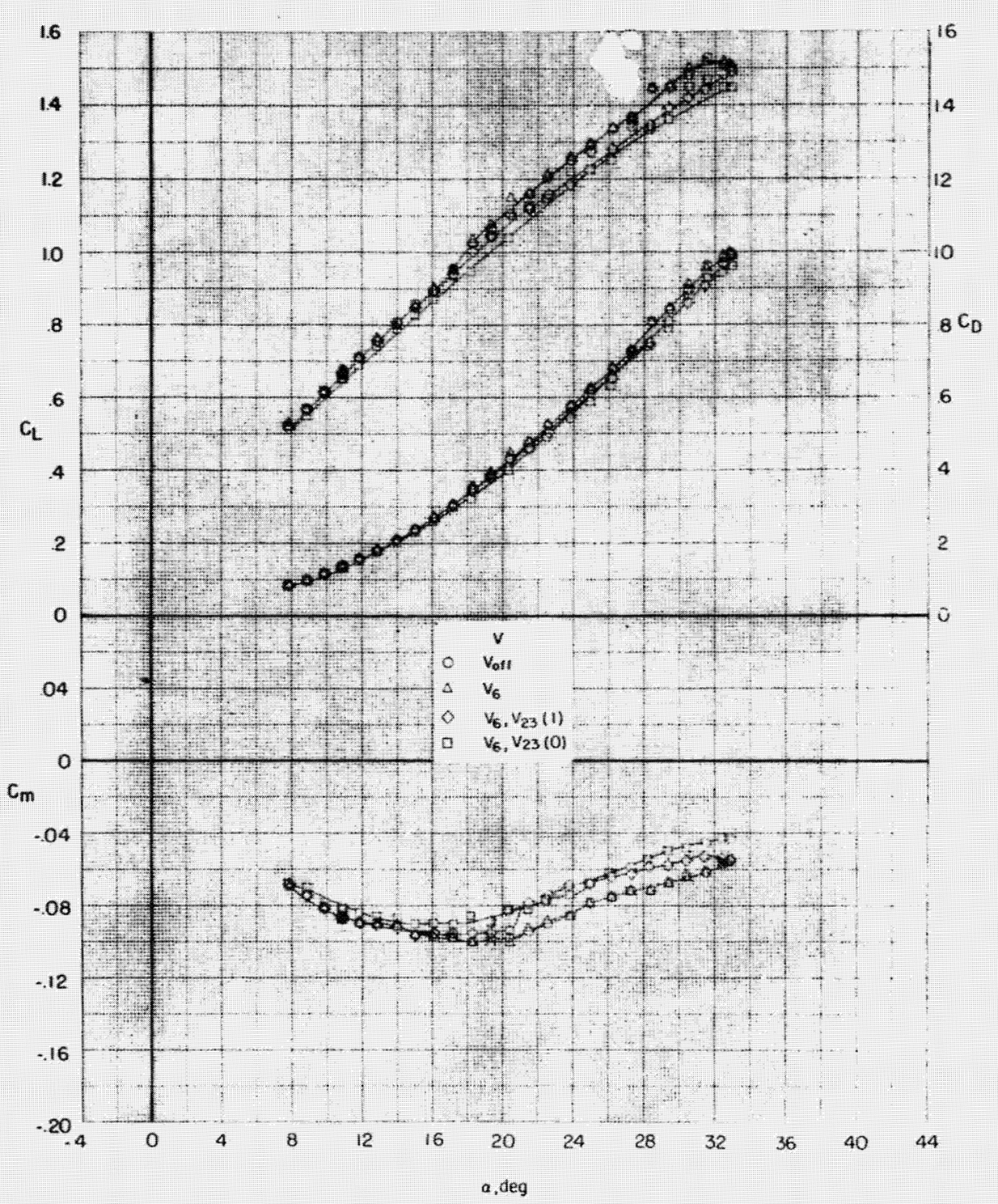

(b) $W_3 = 0^0$

Figure 12.- Continued.

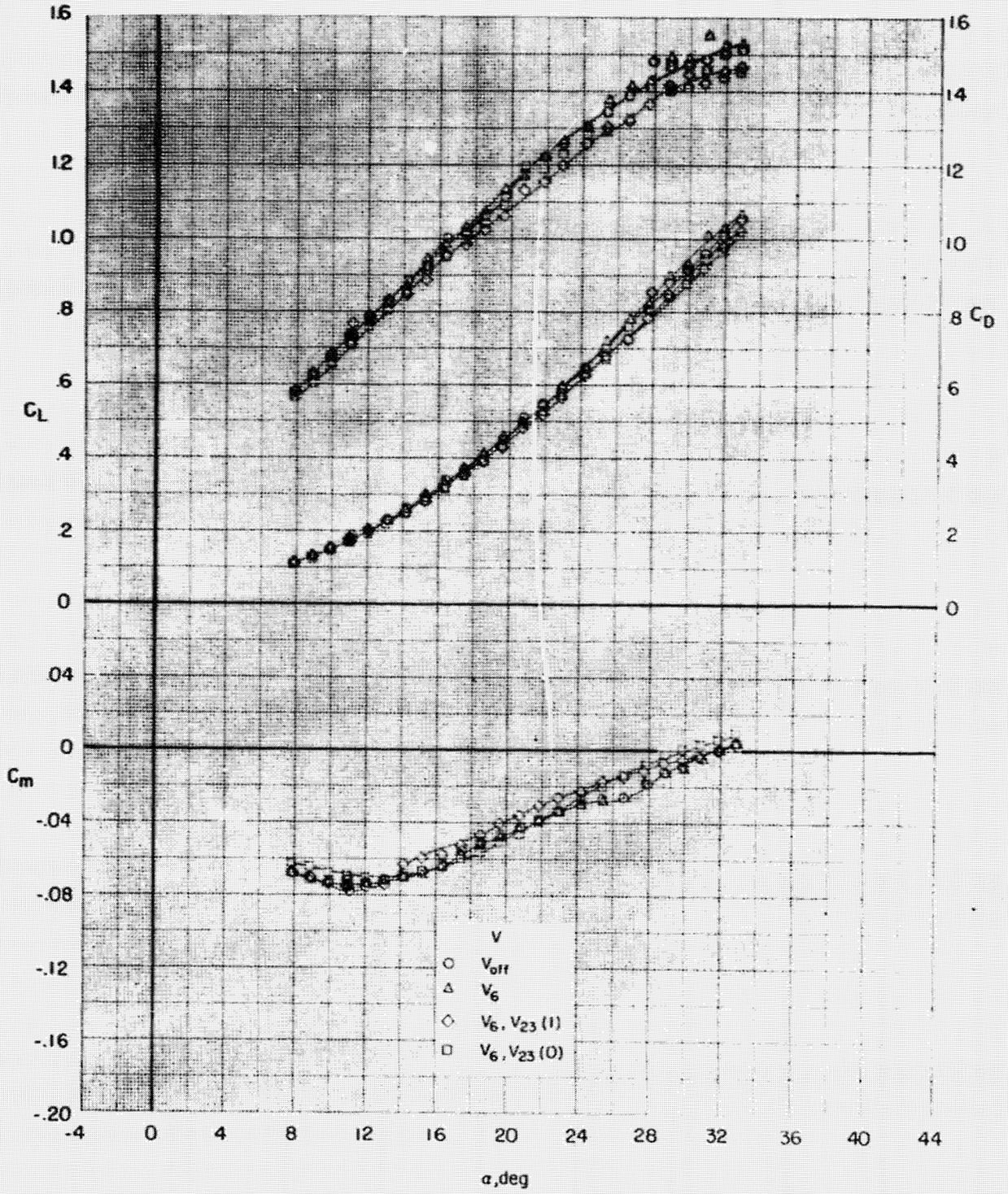

(c) $W_f = 0^0$

Figure 12.- Continued.

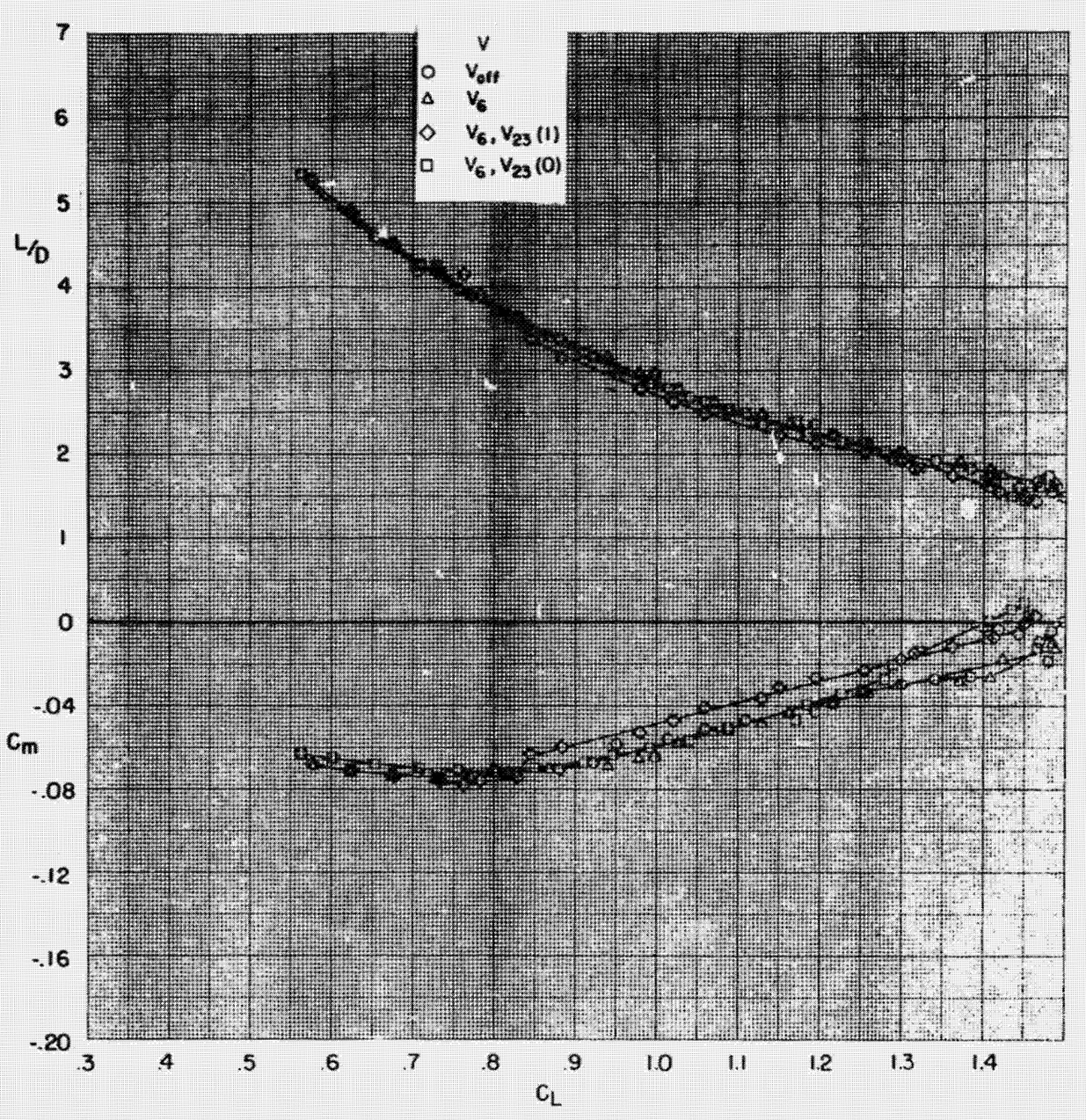

(c) Concluded.
Figure 12.- Concluded.

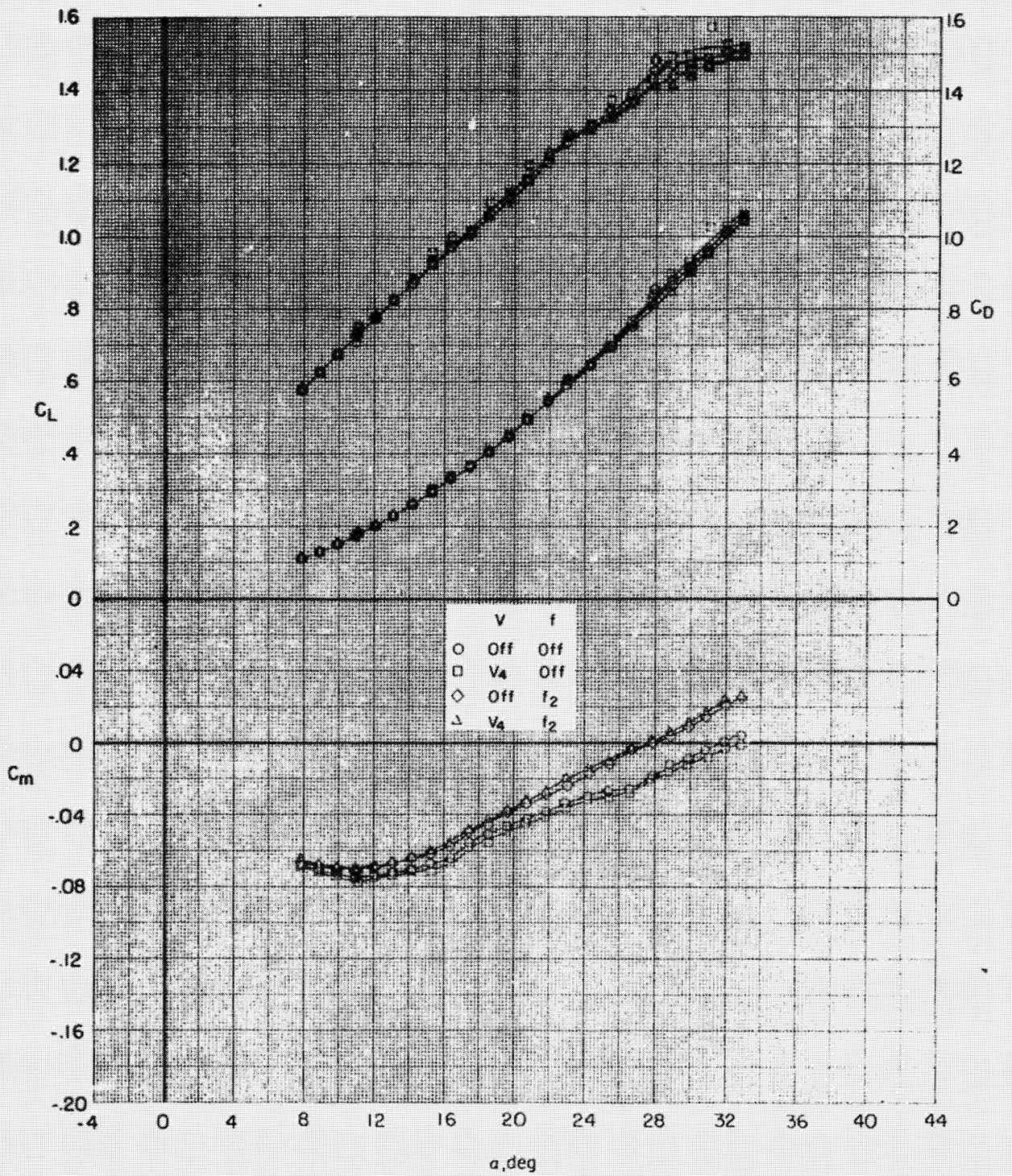

Figure 13.- Effect of vertical tail, V_4, and strake f_2 on the longitudinal characteristics. β =5°, W_f = 0°, V_6, V23 (0)

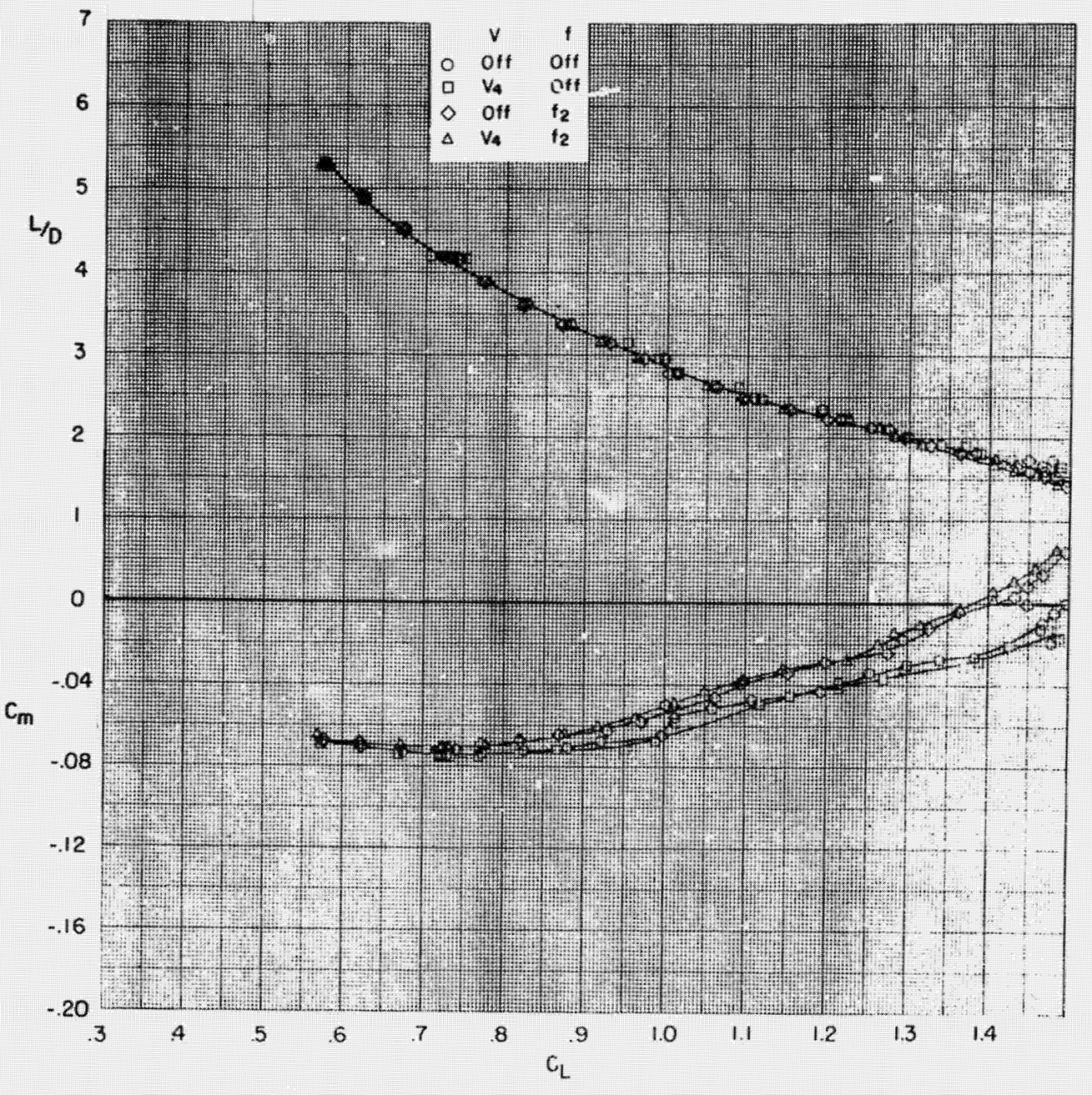

Figure 13.- Concluded.

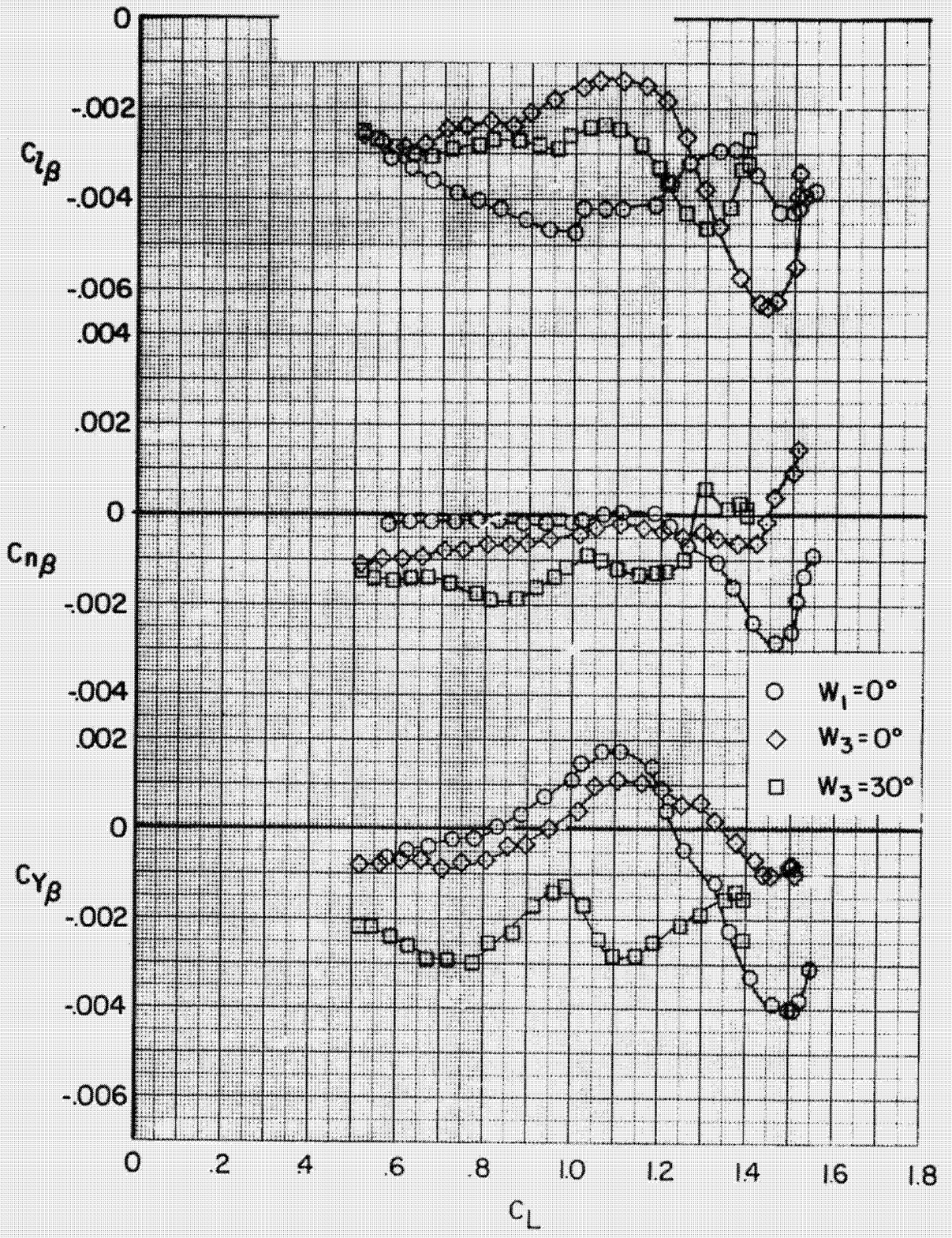

(a) V_{off}

Figure 14.- Effect of wing leading edge configuration on the lateral directional stability parameters.

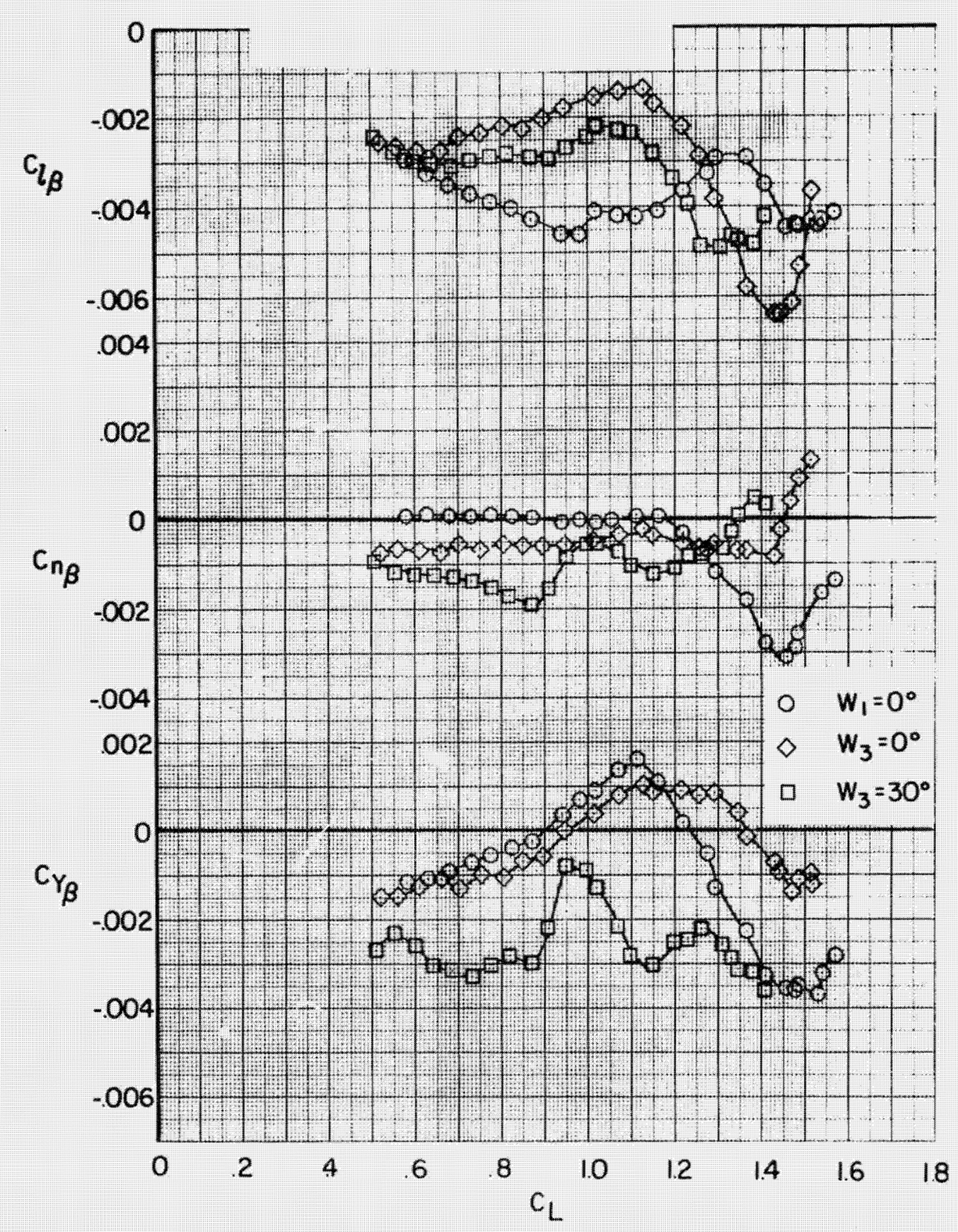

(b) V_6

Figure 14.- Continued.

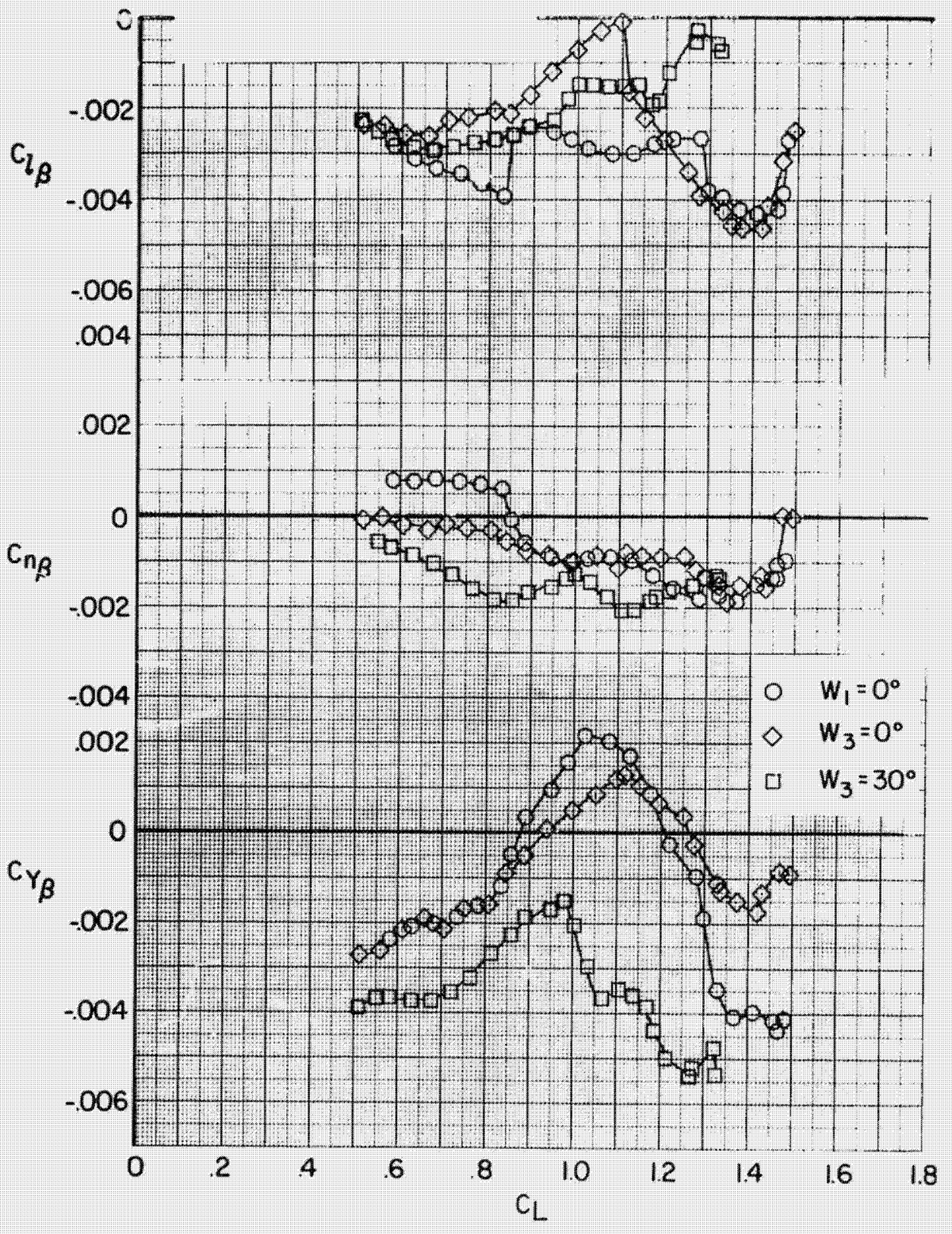

(c) V_6, V_{23} (I)

Figure 14.- Continued.

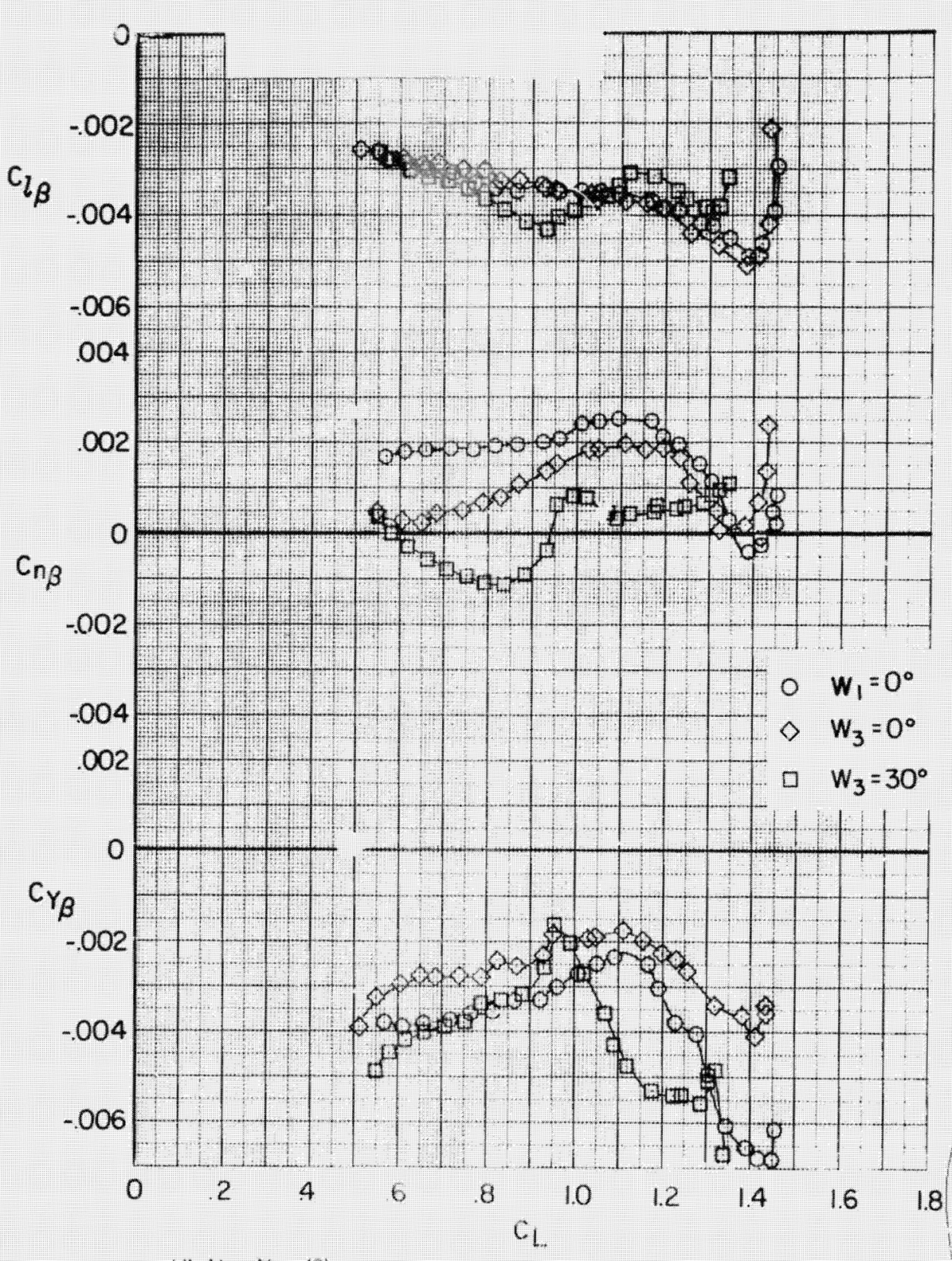

(d) V_6, V_{23} (0)

Figure 14.- Concluded.

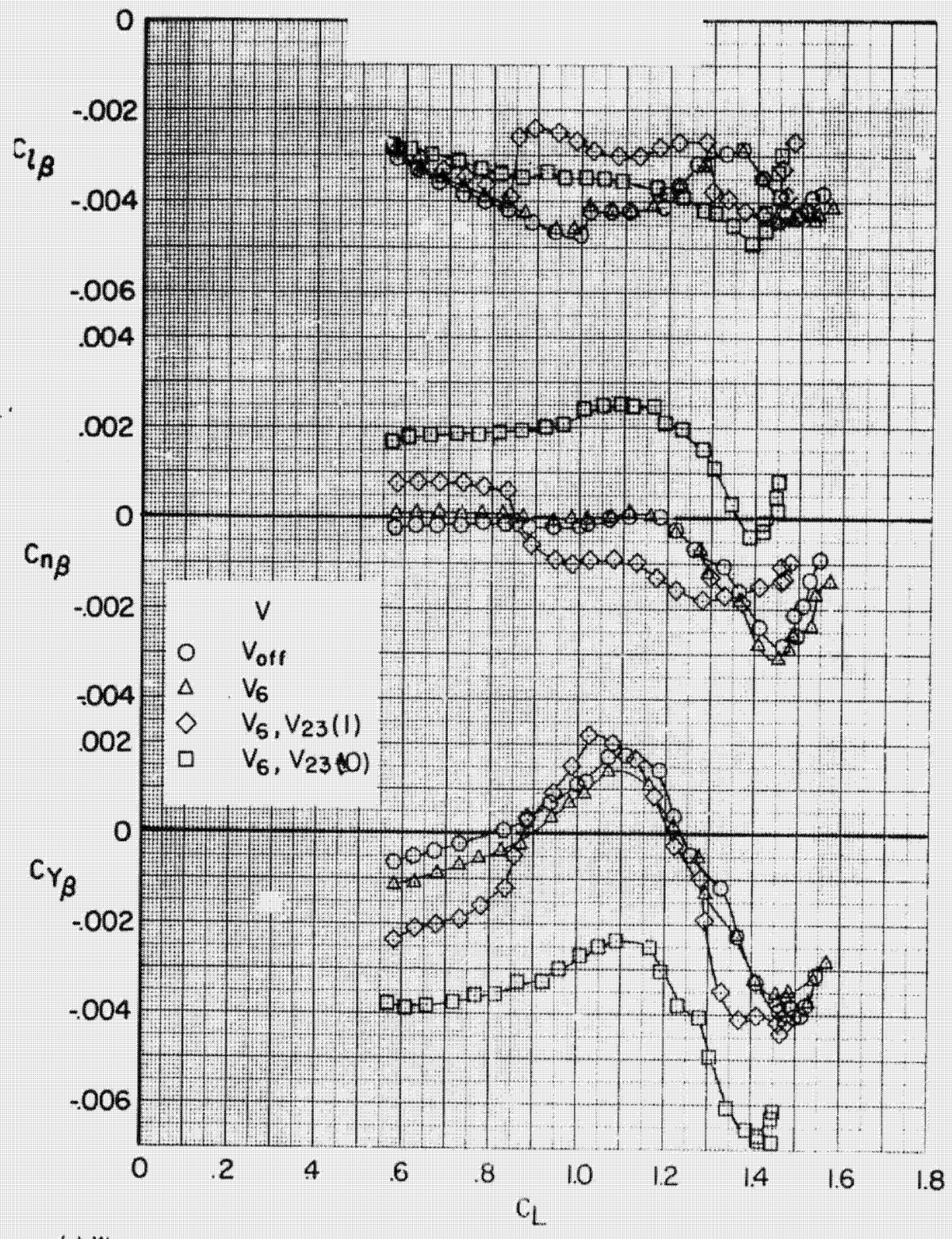

(a) W_1

Figure. 15- Effect of vertical tail configuration on the lateral-directional stability parameters.

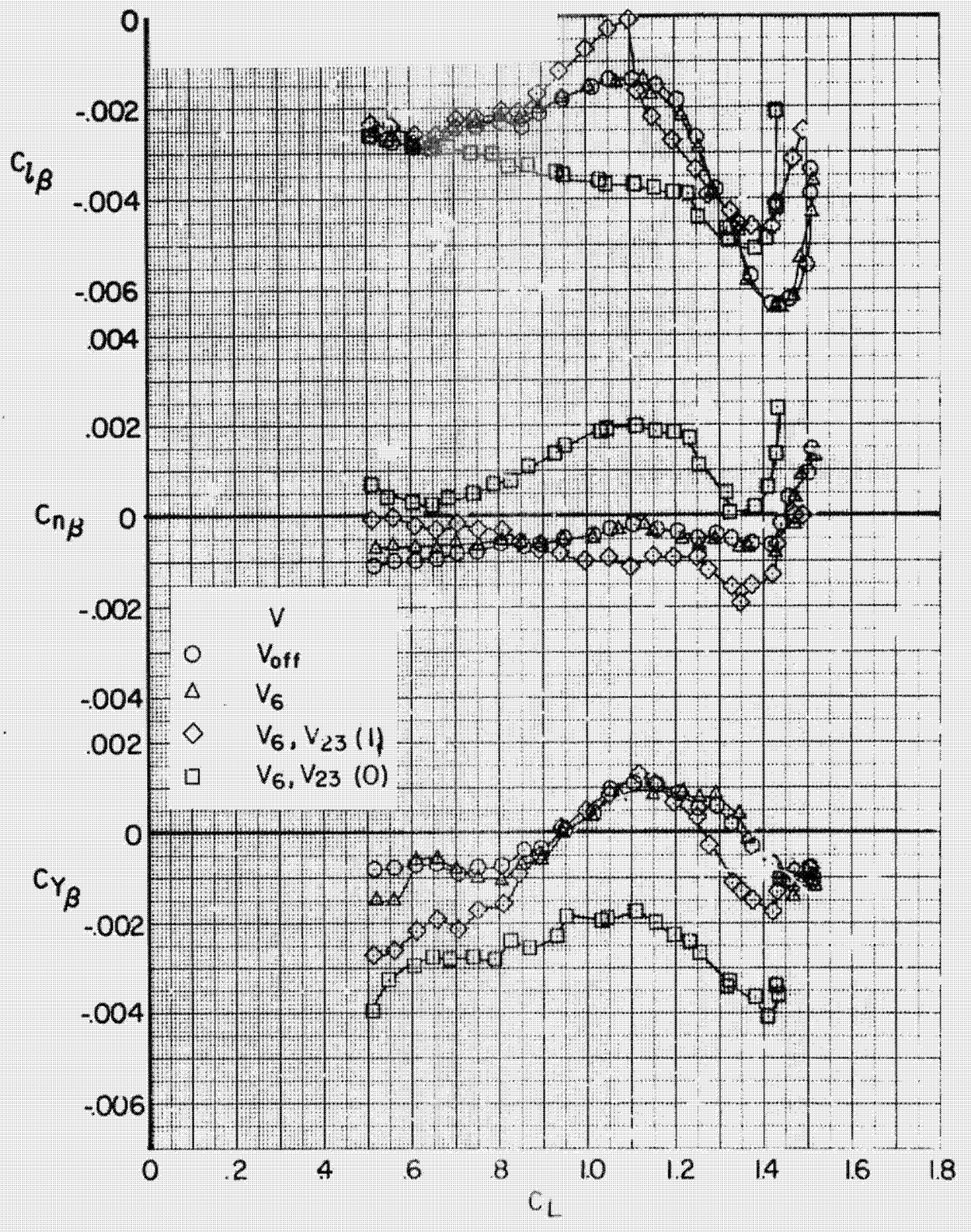

(b) $W_3 = 0^0$

Figure 15 .- Continued.

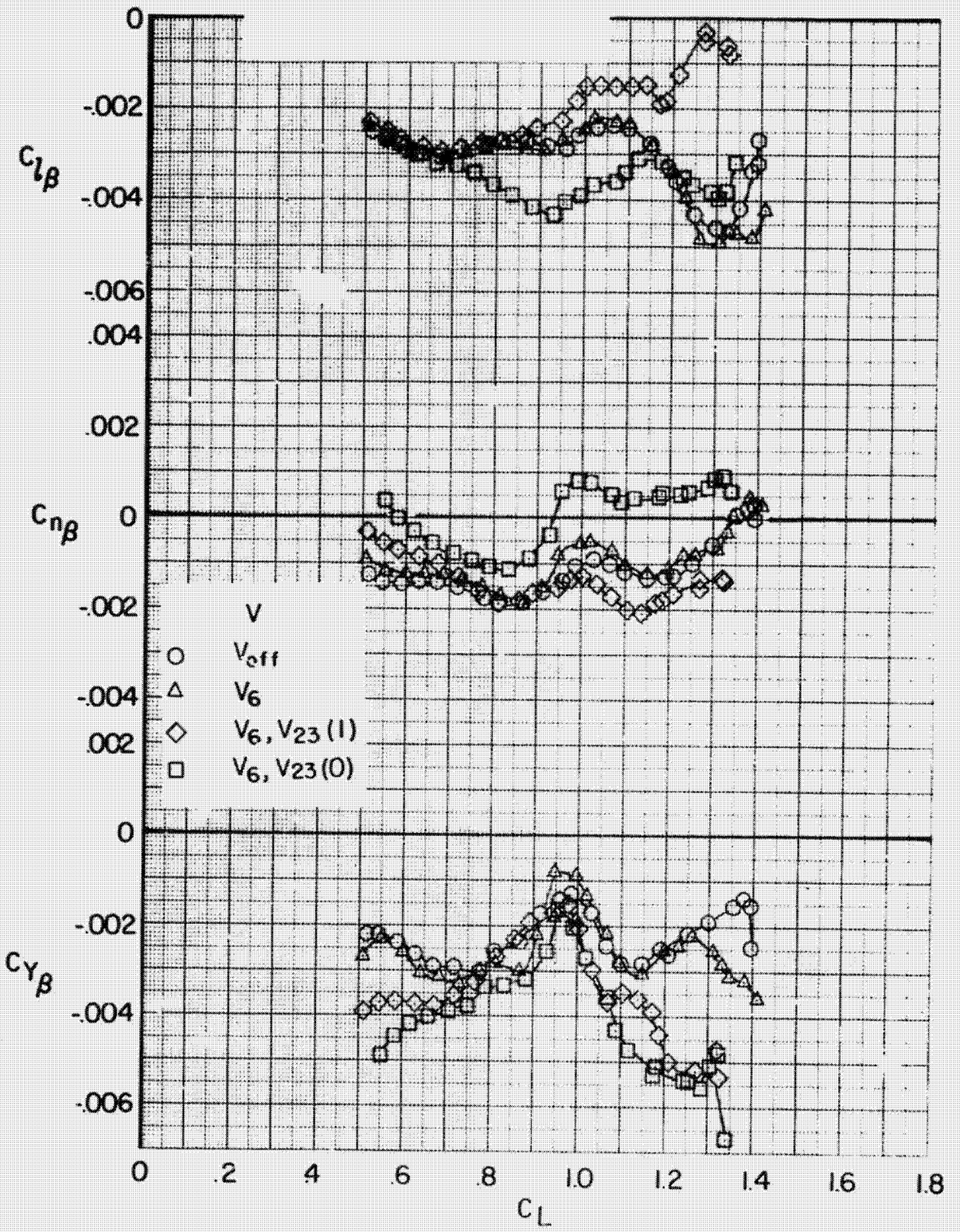

(c) $W_3 = 30^0$

Figure 15.- Concluded.

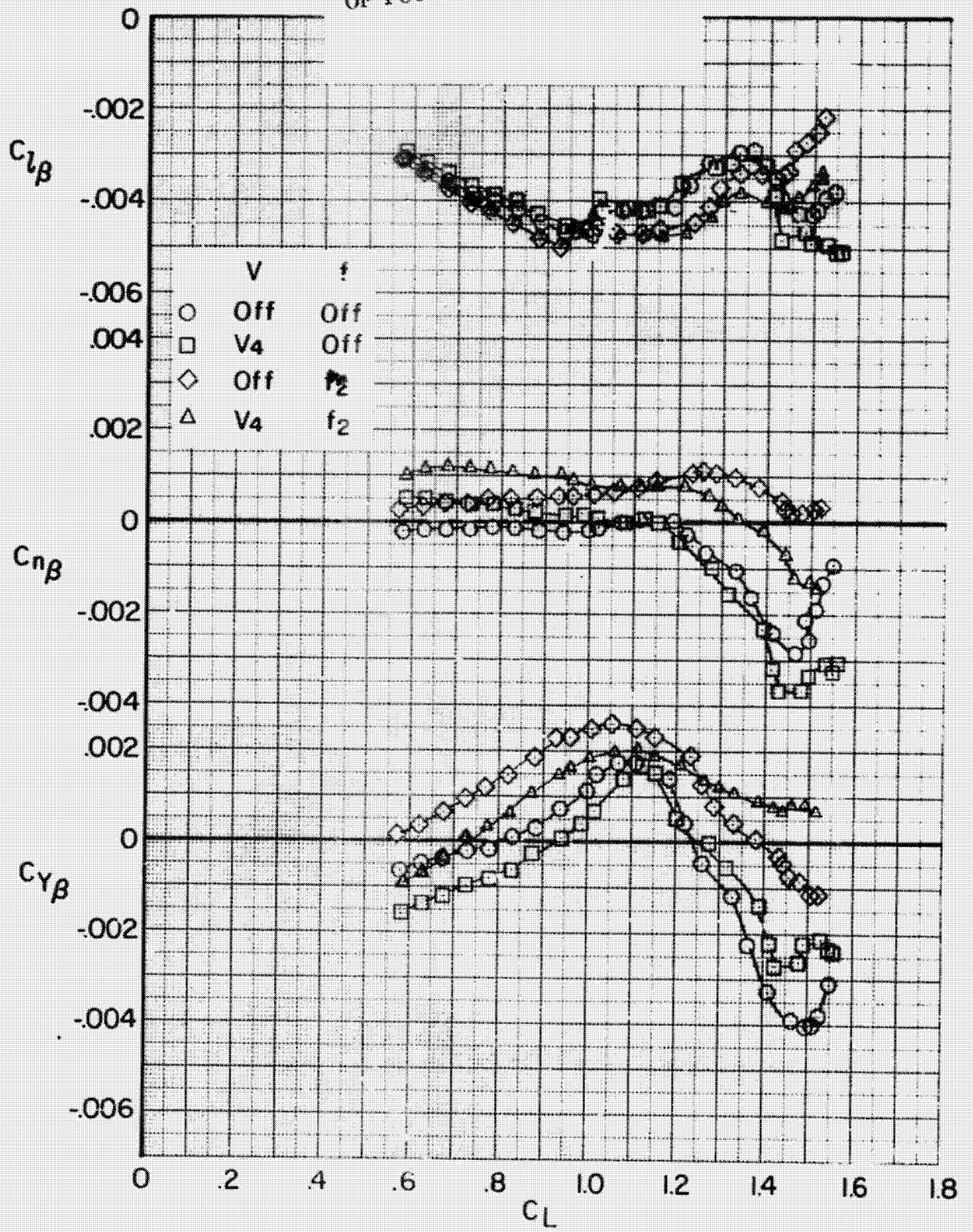

Figure 16.- Effect of vertical tail, V_4, and strake, f_2, on the lateral directional stability parameters. $W_f = 0^0$, V_6, V_{23} (0).

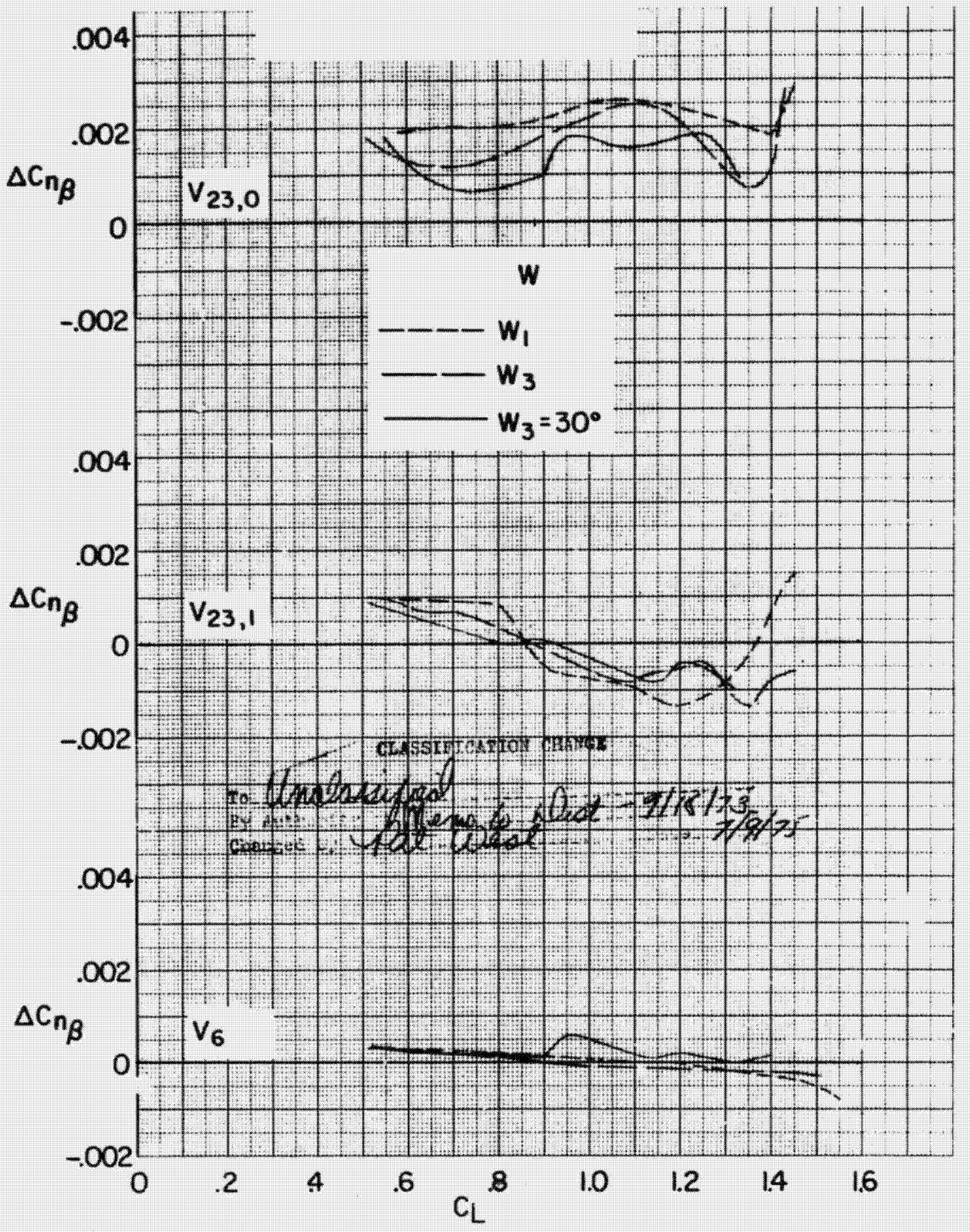

Figure 17.- Effect of wing leading-edge configuration on the contribution of the vertical tails to the directional stability, ΔC_{n_β}.

1. Report No.	2. Government Accession No.	3. Recipient's Catalog No.
NASA TM 78683		

4. Title and Subtitle	5. Report Date
EFFECT OF LEADING-EDGE CONTOUR AND VERTICAL-TAIL CONFIGURATION ON THE LOW-SPEED STABILITY CHARACTERISTICS OF A SUPERSONIC TRANSPORT MODEL HAVING A HIGHLY-SWEPT ARROW WING	March 1978
	6. Performing Organization Code: 3850

7. Author(s)	8. Performing Organization Report No.
Vernard E. Lockwood	
	10. Work Unit No.
9. Performing Organization Name and Address: Langley Research Center, Hampton, VA 23665	11. Contract or Grant No.
	13. Type of Report and Period Covered: Technical Memorandum
12. Sponsoring Agency Name and Address: National Aeronautics and Space Administration, Washington, DC 20546	14. Sponsoring Agency Code

15. Supplementary Notes

16. Abstract

A low-speed investigation has been made on a highly-swept arrow-wing model to determine the effect of wing leading-edge contour and vertical-tail configuration on the aerodynamic characteristics in pitch and sideslip. The investigation was made with the trailing-edge flaps deflected over a range of angles of attack from 8° to 32°. The tests were made at a Mach number of 0.13, which corresponds to a Reynolds number of about 3×10^{6} based on the wing reference chord.

17. Key Words (Suggested by Author(s))	18. Distribution Statement
Leading-Edge Contour Vertical-Tail Configuration Low-Speed Stability	Unclassified - Unlimited Star Category - 02

19. Security Classif. (of this report)	20. Security Classif. (of this page)	21. No. of Pages	22. Price*
Unclassified	Unclassified	38	$4.50

*For sale by the National Technical Information Service, Springfield, Virginia 22161